SUPPLEMENTARY DATA FOR:

Evidence for a Late Cambrian juvenile arc terrane and a buried suture within the Laurentian Caledonides of Scotland: comparisons with hyper-extended Iapetan margins in the Appalachians and Norway

M. Dunk[1], R.A. Strachan[1], K.A. Cutts[2], S. Lasalle[1], C.D. Storey[1], I.M. Burns[3], M.J. Whitehouse[4], M.B. Fowler[1], H. Moreira[1], J. Dunlop[1] & I. Pereria[1]

1. School of Earth & Environmental Sciences, University of Portsmouth, Burnaby Rd, Portsmouth, PO1 3QL.

2. Department of Geology, Universidad Federal de Ouro Preto, Ouro Preto, Brazil.

3. 6, McKenzie Crescent, Bettyhill, By Thurso, Sutherland, KW14 7SY

4. Department of Geosciences, Swedish Museum of Natural History, Box 50 007, SE-104 05, Stockholm, Sweden.

1. Nd analyses

1.1. Sample descriptions

Two samples of amphibolite (IBA1C and IBSP4) and two samples of siliceous gneiss (IBPM10 and IBPM10a) were analysed. Sample IBA1C was collected at NC 27962 96462; sample IBSP4 at NC 28104 96733; samples IBPM10 and IBPM10a at NC 28210 96733. The amphibolites typically comprise a foliated to granoblastic assemblage of hornblende-plagioclase-biotite-quartz with accessory titanite, zircon, ore, cummingtonite, rutile, garnet, epidote and apatite and secondary chlorite and calcite. The siliceous gneisses typically comprise a granoblastic assemblage of quartz-plagioclase-biotite with accessory garnet, amphibole, titanite, allanite and ore.

1.2. Analytical methods

Major element and REE data were obtained by ICPAES at Oxford Brookes University, following rock dissolution by standard fusion and $HF/HClO_4$ procedures. REE were preconcentrated before analysis by standard cation exchange procedures. Other trace elements were analysed by XRF at the British Geological Survey. Natural rock standards, including certified reference materials, were used for all calibrations. Accuracy and precision of the data were estimated at 2-3% rsd for major elements, and 5-10% for trace elements. Data are available in Burns et al (2004).

Isotopic data were acquired at the University of Oxford. Samarium and neodymium were separated from whole-rock powders using standard dissolution and ion-exchange chromatography methods (modified after Eugster et al. 1970). Element concentrations were determined by isotope dilution using a mixed ^{149}Sm and ^{150}Nd enriched tracer prior to dissolution. Isotope ratios were determined using a VG54E single collector thermal ionisation mass spectrometer operated by the ANALYST software of Ludwig (1992). Neodymium isotopic ratios were corrected for within-run mass fractionation by normalisation to a ^{146}Nd/^{144}Nd ratio of 0.7219; replicate analyses of La Jolla standard yielded a mean ^{143}Nd/^{144}Nd ratio of 0.511851 ± 0.000025 (0.005%, 2σ); error on ^{147}Sm/^{144}Nd ratios is c. ± 0.1%. All regression calculations used a ^{147}Sm decay constant of 6.54 x $10^{-12}a^{-1}$ (Lugmair & Marti 1978) and were plotted using Isoplot (Ludwig (1991); all quoted errors are at the 95% confidence level. εNd parameters were calculated relative to CHUR (^{143}Nd/^{144}Nd = 0.512638; ^{147}Sm/^{144}Nd = 0.1966; Jacobsen & Wasserburg 1984). Depleted mantle models used the parameters of De Paolo (1981) and De Paolo et al. (1991).

1.3. Results

Sample	Sm ppm	Nd ppm	144Nd	2 sigma	144Nd	eNd(0)	**eNd(500)**
=========	=========	=========	=========	=========	=========	=========	**=========**
IB A1c	1.815	5.630	0.512970	0.0017	0.1949	6.5	**6.6**
IB PM10	3.588	12.901	0.512775	0.0019	0.1681	2.7	**4.5**
IB PM10a	6.171	20.212	0.512958	0.0029	0.1846	6.2	**7.0**
IB SP4	4.575	14.516	0.512949	0.0026	0.1906	6.1	**6.5**
BCR-1	*6.541*	*28.664*	*0.512616*	*0.0021*	*0.1380*	*-0.4*	3.3

Table 1. Nd isotope data

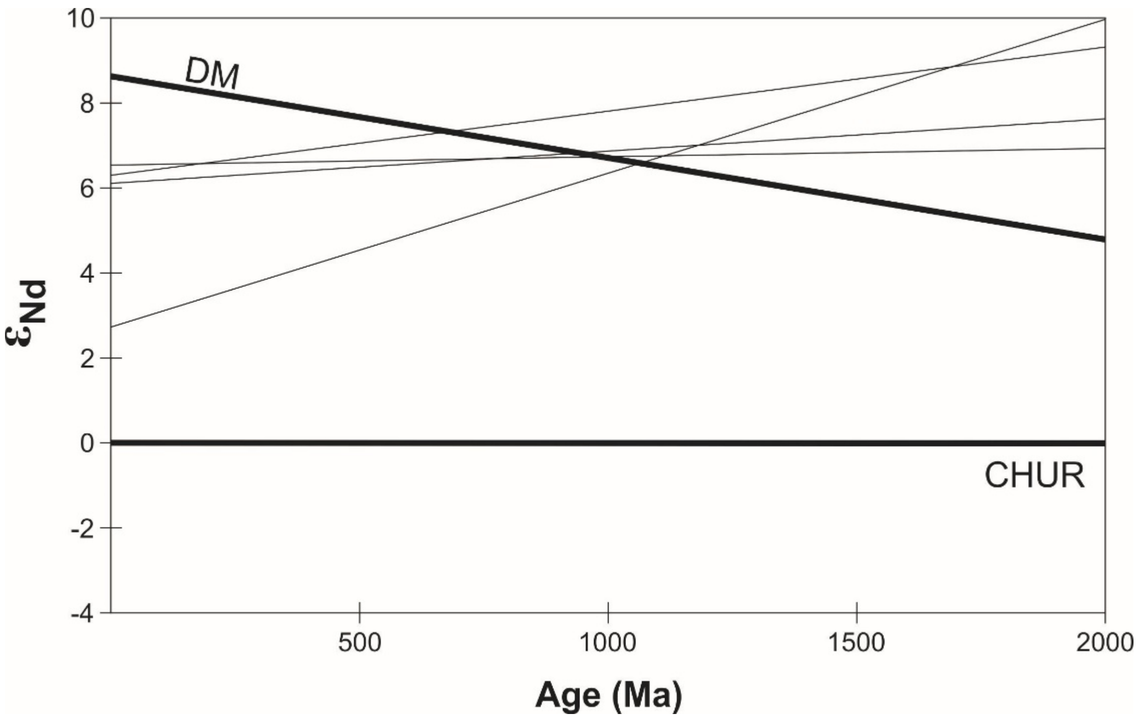

Fig. 1. Nd isotope data

2. U-Pb zircon, monazite and rutile geochronology

2.1. Sample descriptions and petrology

One of three samples of homogenous grey gneiss yielded zircon and monazite, this was collected from a small quarry at NC 8215 6490 (RS-14-16). It is composed of 45% quartz, 35% plagioclase, 10% biotite, 5% magnetite, 3% garnet, 1% K-feldspar, giving it a trondhjemitic composition (Burns, 1994). The weak medium grained gneissic fabric is defined by aligned biotites with elongate quartz featuring embayments and tails. Two weaker foliations are also apparent at c. 40° either side of the main foliation, although due to the lack of defining minerals of each their relative ages are uncertain.

A sample of a very coarse-grained, unfoliated pegmatite within a localised sinistral shear zone was collected from NC 7821 6512 (MD-16-05). It is composed of 40% quartz, 30% plagioclase, 20% K-feldspar and 10% biotite, giving it a granodioritic composition. The sub-vertical shear zone and associated sheet trend c. E-W, cross cutting regional upright folds.

Samples from two weakly foliated pegmatites were collected from a road section at NC 8082 6471 (MD-16-06/07). MD-16-06 is composed of 40% quartz, 30% plagioclase, 20% biotite, 10% K-feldspar with accessory garnet. MD-16-07 is composed of 45% quartz, 35%

plagioclase and 20% biotite with minor K-feldspar and rare garnet. Biotite defines the foliation of both samples with quartz and plagioclase phenocrysts (≤3cm) often aligned to the foliation. The foliation in both samples is parallel to the margins of the intrusions, which cross cut the 'S1' foliation of the host gneisses as well as upright folds.

Sample MD-16-01 was obtained from a garnet-staurolite-sillimanite paragneiss present within a boudin (ca. 6 by 2m) situated in the eastern foundations of the Strathy lighthouse (NC 8282 6964). The foliation preserved in the boudin is subvertical (at c. 90° to the main foliation of the host gneiss) and trends roughly east-west. The rock is medium-coarse grained, foliated and contains garnet, quartz, plagioclase, anthophyllite, biotite, sillimanite, staurolite, spinel, apatite, zircon, rutile, ilmenite and chlorite.

2.2. Analytical methods

Samples were crushed using a hydraulic splitter, jaw crusher and disc mill before being sieved to <500µm. Samples were then put across a Wilfley table, through a Frantz diamagnetic separator and LST Fastfloat heavy liquids (2.80 g/mL). Zircon (RS-14-16, MD-16-05, 06, 07) and monazite (RS-14-16) were picked from the high-density, low-magnetism fraction of the sample using fine tweezers. Grains were mounted in epoxy resin and polished to approximately halfway through the grains to reveal internal structures. Grains were imaged using a combination of two scanning electron microscopes at the University of Portsmouth: Phillips XL30 W filament and Zeiss EVO10MA LaB6 source. The majority of images were taken using backscattered electron (BSE) detection due to a general lack of CL response. These images were used to guide further analysis and all following image descriptions are based on observations in BSE.

U-Pb dating was undertaken by laser ablation inductively coupled mass spectrometry (LA-ICP-MS) using an ASI RESOlution excimer (193mm) laser ablation system coupled with an Analytik Jena Plasma Quant MS Elite ICP-MS. Spot sizes of 9 and 11 µm were used for zircon anaylsis due to the small grain size, fine zoning and high concentrations of inclusions and cracks. Spot sizes of 7, 9 and 11 µm were used for monazite analyses at a fluence of 2 - 2.5 J/cm2 and a repetition rate of 2 Hz. Thorium was not recorded at 11 µm due to high concentrations. Spot sizes of 25 and 30 µm were used for rutile analyses at a fluence of 4

J/cm^2 and a repetition rate of 5 Hz. ^{204}Pb, ^{208}Pb and ^{232}Th were monitored to detect the presence of initial Pb.

	Zircon	Monazite	Rutile
ICP-MS			
Type of ICP-MS	Quadrupole		
Brand and model	Analytik Jena Plasma Quant MS Elite		
Gas Flows			
Plasma (impure Ar)	10 L/min	10 L/min	10 L/min
Auxiliary flow (Ar)	1.65 L/min	1.65 L/min	1.65 L/min
Nebulising flow (Ar)	0.90 - 0.92 L/min	0.89 - 0.91 L/min	0.90 - 0.92 L/min
Carrier (He)	300 mL/min	300 mL/min	300 mL/min
Nitrogen (N)	3 mL/min	3 mL/min	3 mL/min
Laser			
Type of laser	ArF excimer		
Brand and model	ASI RESOlution excimer (193mm)		
Wavelength	193 nm	193 nm	193 nm
Spot size	9 and 11 µm	7 and 11 µm	30 and 25 µm
Rep. rate	3/2 Hz	2 Hz	5 Hz
Fluency	4 -3 J/cm^2	2 -2.5 J/cm^2	4 J/cm^2
Data acquisition parameters			
Scanned masses	202, 204, 206, 207, 208, 232, 235, 238	202, 204, 206, 207, 208, 232, 235, 238 (232 not collected at 11 µm)	202, 204, 206, 207, 208, 232, 235, 238
Settling time	0.001 s		
Sample time	0.01, 0.02 (for 206), 0.03 s (for 207)	0.01, 0.02 (for 206), 0.03 s (for 207)	0.01, 0.02 (for 206), 0.03 s (for 207)
Number of runs	12	7	2
Detector mode	Counting		
Deadtime	20 ns		
Background collection	25 s		
Ablation	30 s		
Washout	15 s		

Table 2. Detailed LA-ICP-MS parameters

Plešovice zircon (Sláma et al., 2008) was used as a primary standard for zircon dating, with BB9 (Santos et al., 2017) and 91500 (Wiedenbeck et al., 1995) zircons as secondary standards. Zircon standards Temora (Black et al., 2003) and GJ1 (Jackson et al., 2004) were also used to check for accuracy. Trebilcock monazite (Tomascak et al., 1996) was used as a primary standard for monazite dating, with KMO (MacLachan et al., 2004; Goudie et al., 2014), Bananeiro and Itambé (Gonçalves et al., 2016) monazites as secondary standards. R10 rutile (Luvizotto et al., 2009, Zack et al., 2011) was used as a primary standard for dating rutile, with R19 (Luvizotto et al., 2009, Zack et al., 2011), R13 (Luvizotto et al., 2009) and SAE (C. Lana, pers. comm.) used as secondary standards. Data processing was conducted using Iolite (Paton et al., 2011) and plotted in Excel using the IsoPlot plugin (Ludwig 2003). Discordance was calculated using (1 - $^{206}Pb/^{238}U$ / $^{207}Pb/^{235}U$) x 100.

Forty-nine of 57 analyses of BB9 yield a Concordia age of 559.8 ± 1.5 Ma which is within error of the TIMS age 561 ± 0.83 Ma (Santos et al., 2017; Lana et al., 2017). Seventeen of 59 analyses of 91500 yield a Concordia age of 1059.8 ± 5.1 Ma, which is within the expected range, 1059.2 - 1065.2 Ma (Santos et al., 2017). Eighteen of 36 analyses yield a Concordia age of 414.8 ± 1.9 Ma, which is within error of the TIMS age 416.8 ± 1.1 Ma (Black et al., 2004; Santos et al., 2017). Twenty-four of 36 analyses of GJ1 yield a concordia age of 598.6 ± 1.8 Ma, which is within the expected range, 596.2 - 602.7 Ma (Jackson et al., 2004; Santos et al., 2017).

Thirty-nine analyses on 15 monazite grains from sample RS-14-16 were performed in three U-Pb sessions. When using the Iolite software for data processing of the first two runs at 7µm, the VizualAge_UcomPbine Data Reduction Scheme was applied (Chew et al., 2004) due to variable common Pb reported in the primary standard. Lead isotopic composition was calculated based on multiple K-feldspar analyses from the Trebilcock pegmatite acquired by Tomascak et al. (1996). The third run was undertaken at 11µm and the U-Pb_Geochronology Data Reduction Scheme was applied for this run as Th was not recorded (Paton et al., 2011). Secondary standards for the three runs yielded Concordia and Intercept ages within 1 and 1.5% error compared to the published values of c. 508 Ma for Itambé (Gonçalves et al., 2016) and 1822 ± 2 for KMO monazite (MacLachan et al., 2004).

Seven of 10 analyses of R19 yield a Concordia age of 495.6 ± 6.3 Ma which is within error of the TIMS age of 493 ± 10 Ma (Luvizotto et al., 2009; Zack et al., 2011). Five of 8 analyses of R13 are concordant and yield a concordia age of 509.1 ± 7.9 Ma which is within error of the SIMS age of 504 ± 4 Ma (Luvizotto et al., 2009). All 34 analyses of SAE are concordant and yield a concordia age of 508.8 ± 3.7 Ma, which is outside of the TIMS age of 495 (pers comm, C. Lana, University of Ouro Preto) although the University of Portsmouth usually obtains an age of c. 505 Ma. Six of 15 analyses of R632 yield a Concordia age of 510 ± 8 Ma, compared to the LA-ICP-MS age of 496 ± 2 Ma (Axelsson et al., 2018). It is common for sets of secondary standards analysed by LA-ICP-MS to have an offset for 1.5% to TIMS ages, attributed to several pieces of zircon over several runs on multiple days (e.g. Gehrels et al., 2008; Frei & Gerdes, 2009).

2.3. Accessory minerals characteristics and results

2.3.1 Zircon

Zircon grains from sample RS-14-16 (grey gneiss of Strathy Complex) are subhedral to anhedral in form and range from 60 - 200 µm in length with aspect ratios from 1:1 to 1:6. Care was taken during analysis as many grains exhibit 'patchy' textures, thought to be caused by metamictisation either during hydrothermal alteration (Burns et al., 2004) or high-grade metamorphism. The grains typically have many inclusions (usually apatite, xenotime, monazite), particularly around the edges, thought to be caused by hydrothermal alteration late in zircon formation. Twenty-six of 46 analyses are <15% discordant, with ages ranging from 522 Ma to 383 Ma. Eleven analyses form a cluster giving a concordia age of 503 ± 2 Ma (Fig. 2), with two slightly older grains (not included in the concordia age) at ca. 522 Ma. These two older grains have sector zoning (Fig 3) and can be explained by a number of means, such as uranium gain (e.g. Seydoux-Guillaume et al., 2015), being part of an early stage magma crystallisation or mixing (antecrysts or xenocrysts) (e.g. Miller et al., 2007) or that they represent the minimum age of the complex while the other c. 503 Ma grains have suffered lead loss (e.g. Geisler et al., 2002). A weighted mean average of grains older than 485 Ma rejects the oldest grain (95% confidence level) and yields an age of 504.5 ± 4.7 Ma (Fig 4), which is within the uncertainty of the concordia age. Therefore, we choose to present the Concordia age discounting the aforementioned oldest grain, two grains with large errors and one grain due to mixing of core and rim (CL textural control-based; Fig. 3). This results in the best estimation of the rock at c. 503 Ma, which we interpret as the crystallisation age of the complex. The proposed tectonic model is still valid if the oldest grain represents the minimum age of the complex. A spread of ages from 468 Ma to 425 Ma was also recorded from metamict cores and rims with one rim measurement younger than this at 383 ± 5 Ma.

Fig. 2. U-Pb Concordia diagram for zircon analyses from sample RS-14-16, inset showing sample zircon grains, locations of laser pits and corresponding ages.

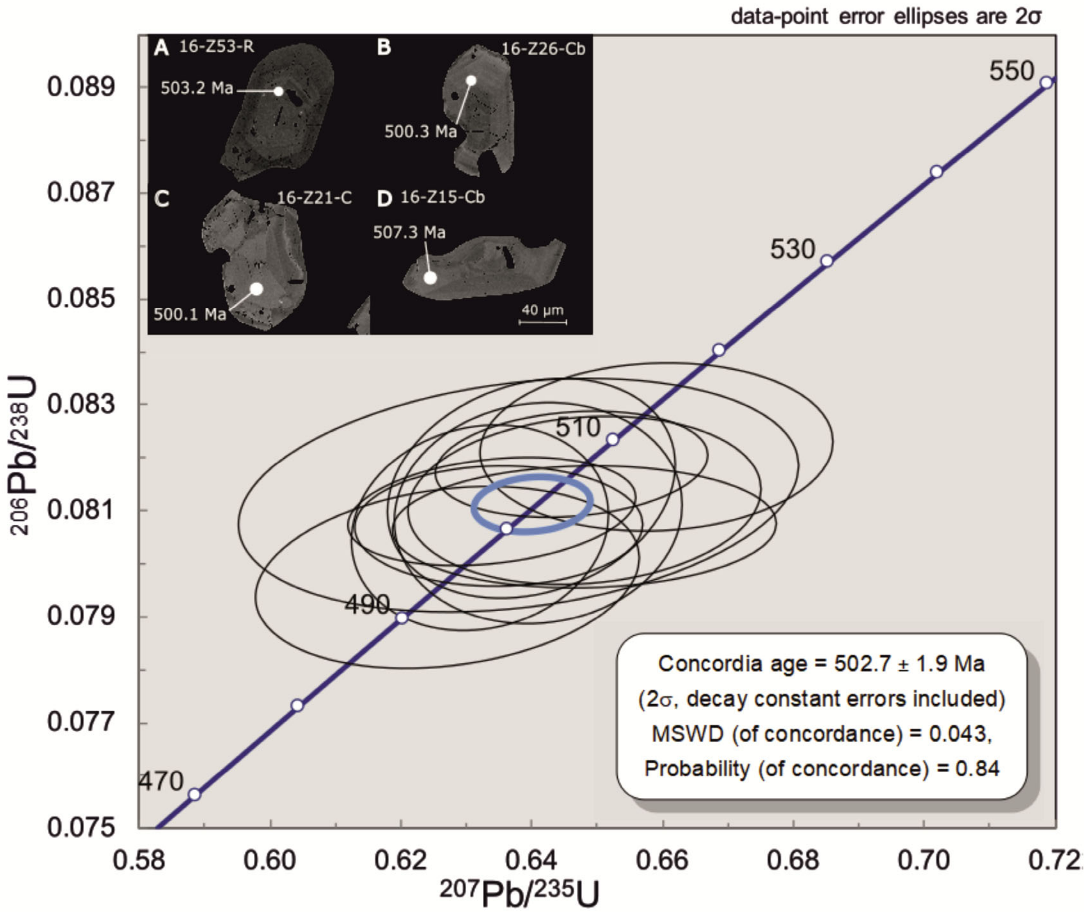

data-point error ellipses are 2σ
A 16-Z53-R
503.2 Ma
B 16-Z26-Cb
500.3 Ma
C 16-Z21-C
500.1 Ma
D 16-Z15-Cb
507.3 Ma
40 μm
550
530
510
490
470
0.089
0.087
0.085
0.083
0.081
0.079
0.077
0.075
0.58
0.60
0.62
0.64
0.66
0.68
0.70
0.72
206Pb/238U
207Pb/235U
Concordia age = 502.7 ± 1.9 Ma
(2σ, decay constant errors included)
MSWD (of concordance) = 0.043,
Probability (of concordance) = 0.84

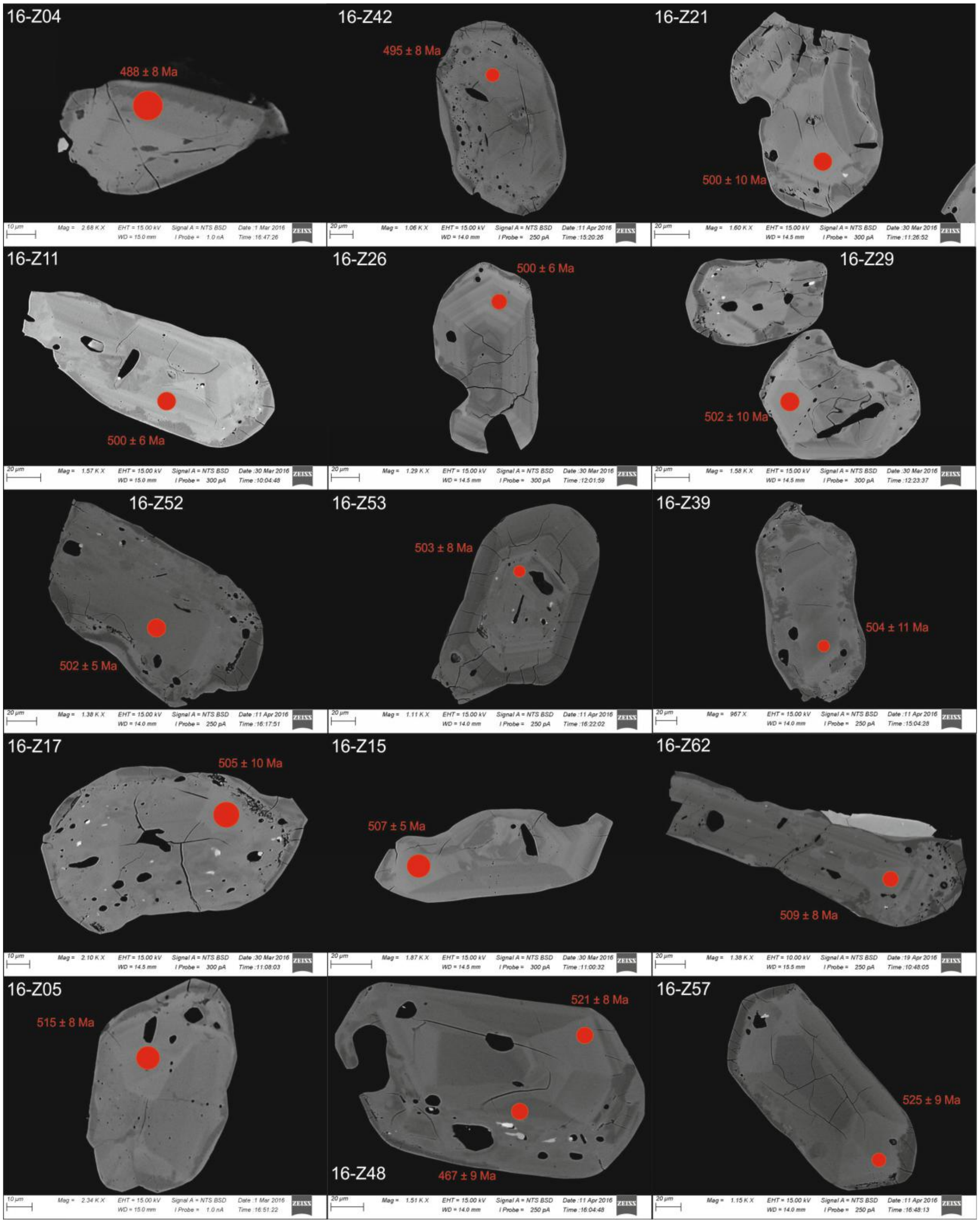

Fig. 3. Backscatter SEM images showing the zircon grains, spot locations and associated ages >485 Ma ($^{206}Pb/^{238}U$). One age of <485 Ma is included as it was located on the same grain.

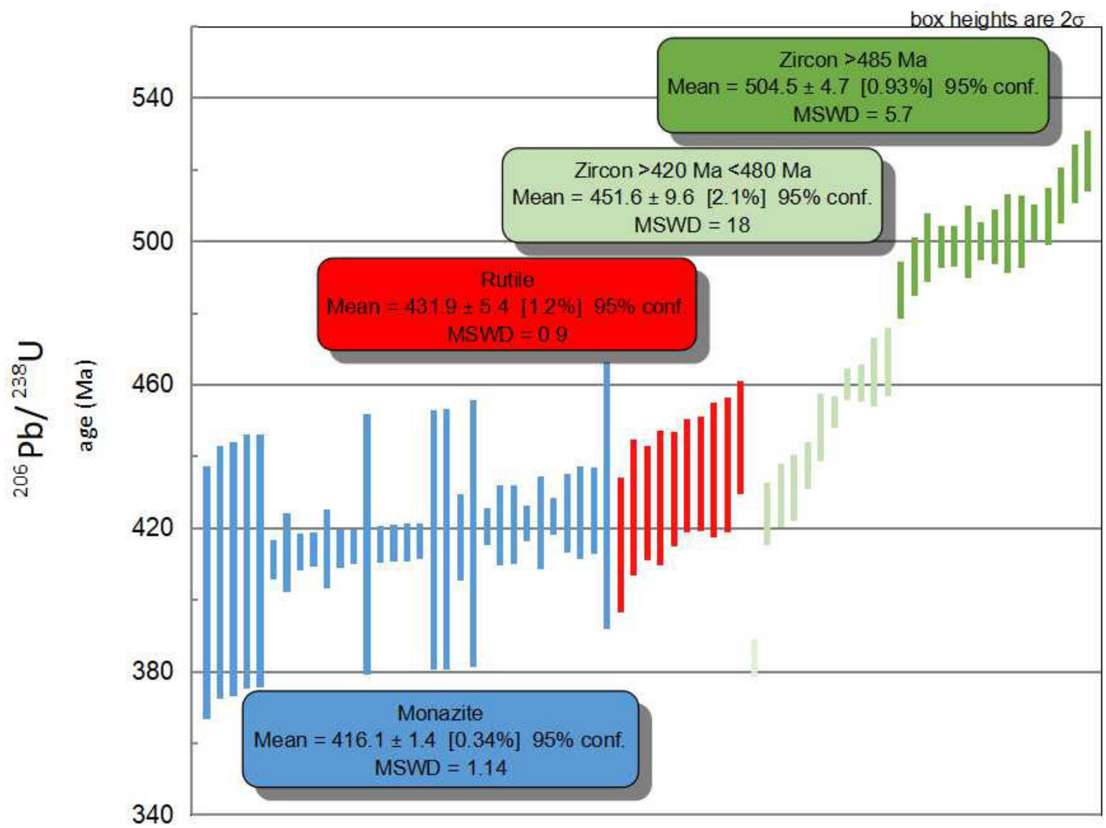

Fig. 4. Compilation graph showing weighted average calculations of each group of analyses. The oldest zircon age was eliminated by Isoplot due to being outside 95% confidence limits.

Sample MD-16-05 (pegmatite within dextral shear zone) contains zircon grains that are usually euhedral prisms 80 - 300 µm in length with aspect ratios from 1:2 to 1:7. Some grains preserve small (<10µm diameter), possibly resorbed cores with a high concentration of inclusions; these areas were therefore not analysed. Other grains have homogenous to weakly oscillatorily zoned cores. Most grains have a sector zoned overgrowth and a homogenous to weakly oscillatorily zoned outer rim. Nine of 24 analyses are <16% discordant. Eight analyses have a spread of ages from c. 470 ± 11 Ma to c. 422 ± 9 Ma, with one younger rim at 395 ± 8 Ma (Fig. 5).

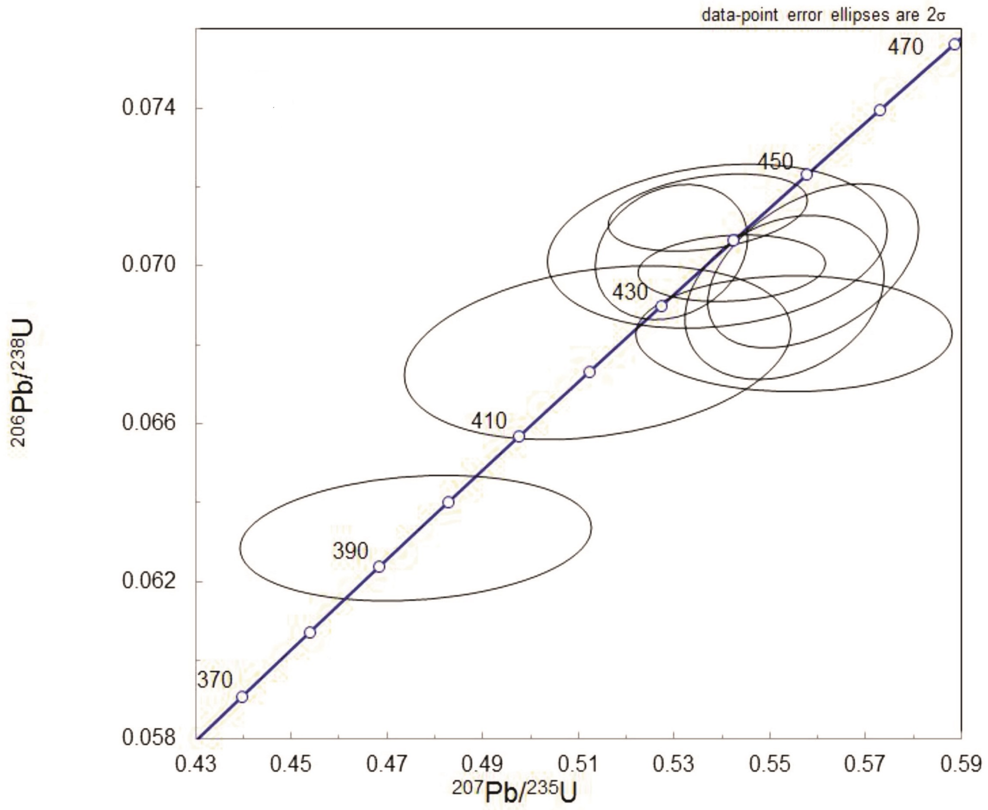

Fig. 5. U-Pb Concordia diagram for zircon analyses from MD-16-05.

Zircon from samples MD-16-06 and MD-16-07 have near identical characteristics so are therefore described together. The zircons are euhedral to subhedral prisms 60 - 200 µm in length with aspect ratios from 1:2 to 1:5. Grains sometimes preserve small (<20µm), possibly resorbed, inclusion-rich cores as in sample MD-16-05; these areas were not analysed. There are two other core types: homogenous and 'patchy'. Most grains have thick oscillatory zoned areas overgrowing the core and sometimes have a thin (<10µm) outer growth. In sample MD-16-06 12 of 24 analyses are <16% discordant. These grains yield a range of ages from c. 469 ± 11 Ma to c. 414 ± 7 Ma (Fig. 6). In sample MD-16-07 15 of 24 analyses are <15% discordant. A range of ages were recorded, from c. 463 ± 5 Ma to c. 411 ± 6 Ma (Fig. 7).

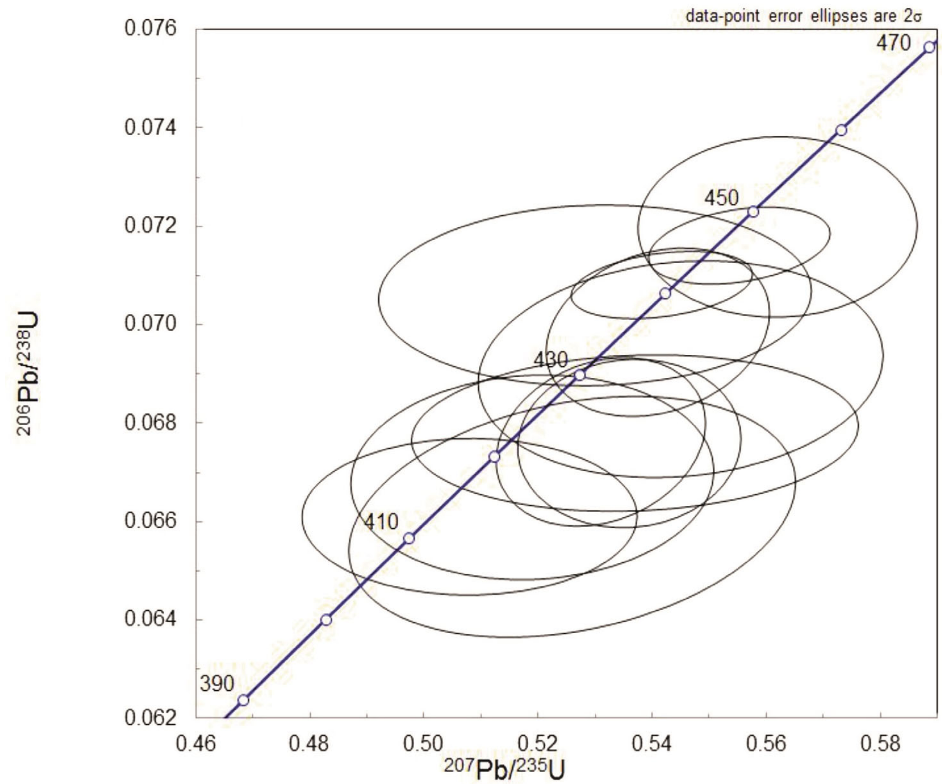

Fig. 6. U-Pb Concordia diagram for zircon analyses from sample MD-16-06.

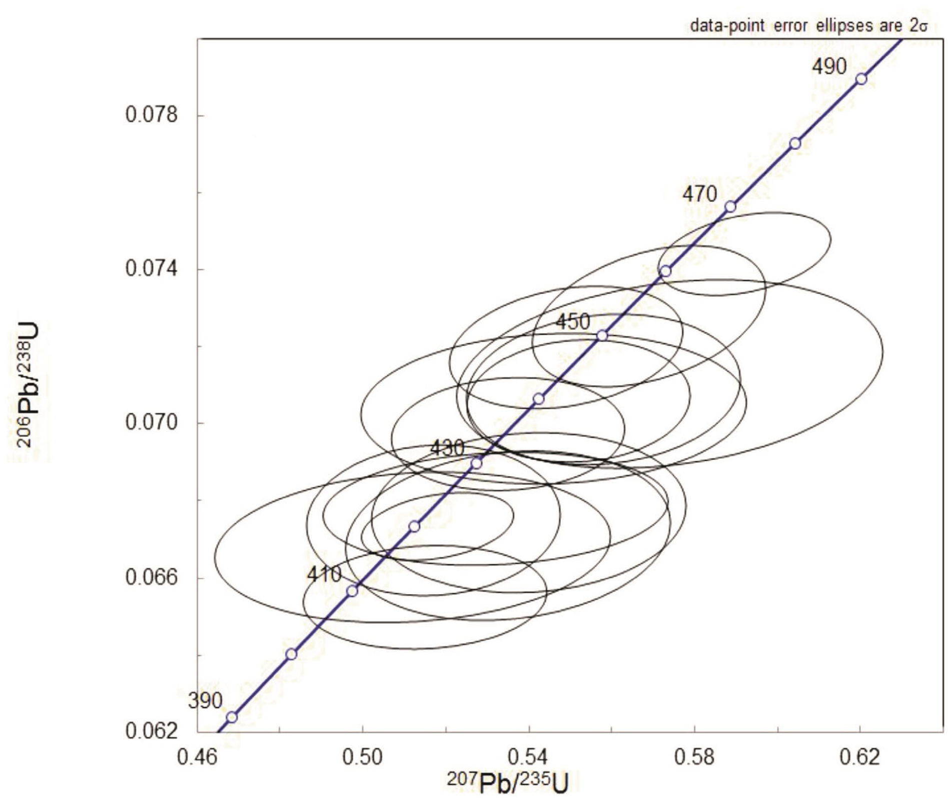

Fig. 7. U-Pb Concordia diagram for zircon analyses from sample MD-16-07.

2.3.2. Monazite

RS-14-16 yields pale yellow anhedral to subhedral monazites 60 – 80 µm in length, with aspect ratios from 1:1.5 to 1:5. Grains range from homogenous to patchy and usually contain <5µm inclusions of apatite. No rims were observed. The first two sessions used 7 µm spot size and show a Concordia age of 422.1 ±3.3 Ma using 20 out of 24 analyses. The third run used 11 µm spot size and consisted of 15 analyses. Of those, 12 yielded a Concordia age of 416.5 ± 2.0 Ma. Between all three runs thirty-two of 39 analyses on 15 grains are concordant, with a range from 401 Ma to 469 Ma, which together yield a Concordia age of 417.3 ± 1.5 Ma (Fig. 8). The difference of precision between the two acquisition parameters (7 and 11 µm) is interpreted as a result of signal intensity. The counts per second are more than two times higher for all the masses acquired when ablated with the bigger spot size.

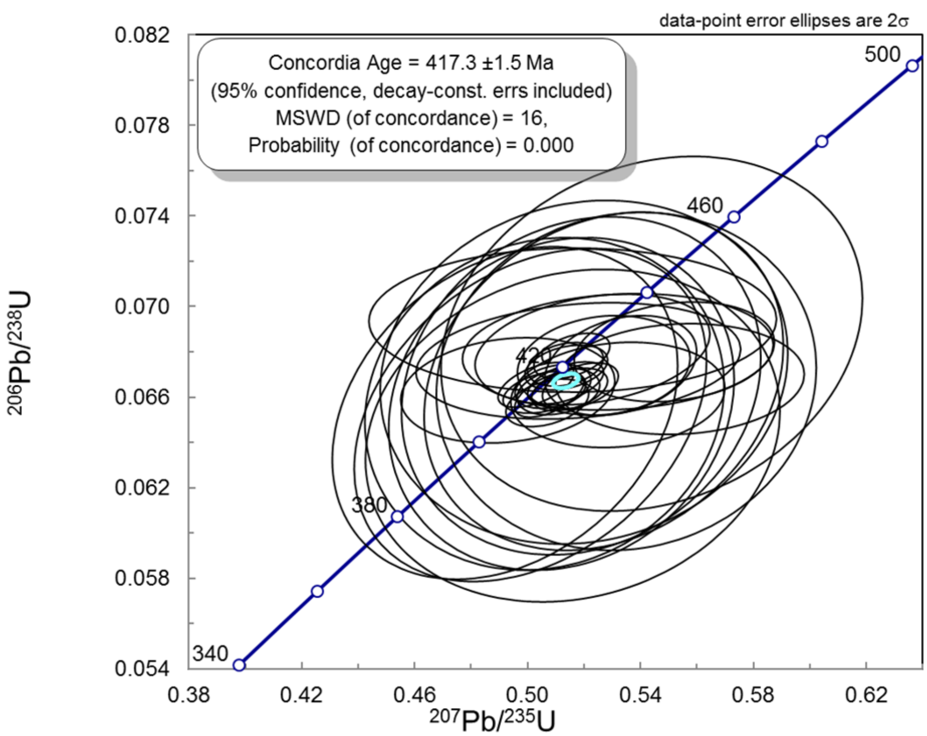

Fig. 8. U-Pb Concordia diagram from monazite analyses from sample RS-14-16.

2.3.3. Rutile

MD-16-01 yields yellowish orange subhedral to euhedral rutiles 40 – 150 µm in length, with aspect ratios from 1:2 to 1:6. Grains are mostly homogenous with some showing a patchy texture, with common <10µm inclusions of zircon. Ten of 16 analyses are <5% discordant, which together yield a concordia age of 433 ± 5 Ma (Fig. 9). The discordant analyses have high levels of common lead, whereas the concordant data points have negligible levels.

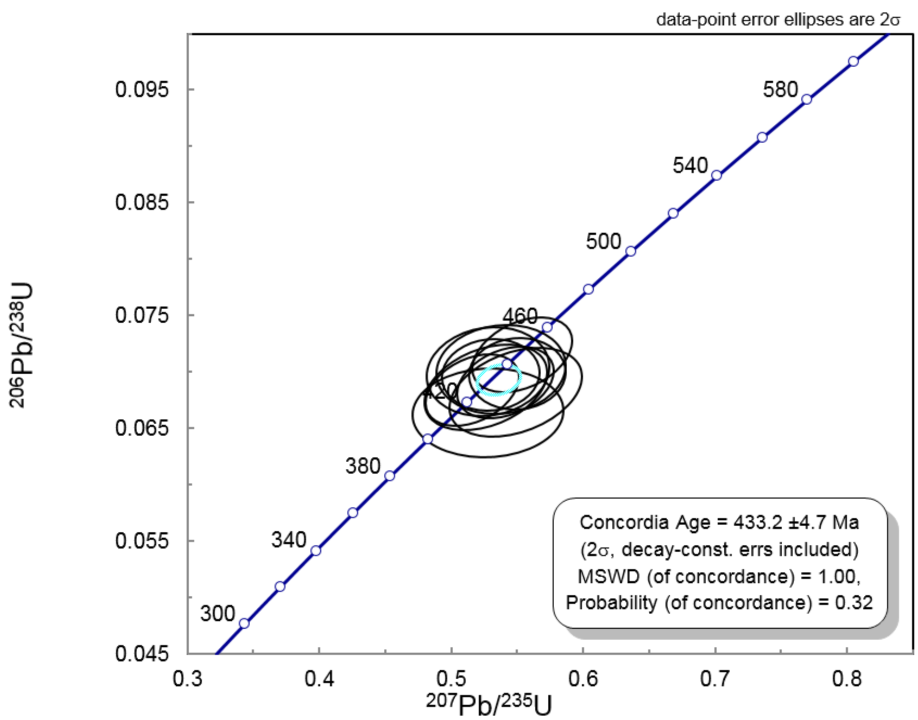

Fig. 9. U-Pb Concordia diagram for rutile analyses from sample MD-16-01.

Sample number:	Zircon	Monazite	Rutile
RS-14-16 (grey gneiss)	**503 ± 2 Ma**	**422 ± 3 to 417 ± 2 Ma**	
MD-16-01 (paragneiss)			**433 ± 5 Ma**
MD-16-05 (pegmatite)	**470 ± 11 Ma to 395 ± 8 Ma**		
MD-16-06 (pegmatite)	**469 ± 11 Ma to 414 ± 7 Ma**		
MD-16-07 (pegmatite)	**463 ± 5 Ma to 411 ± 6 Ma**		

Table 3. Summary of U-Pb data and results from accessory minerals

3. Hafnium analyses

Hafnium isotope ratios were measured by laser ablation multi-collector inductively coupled plasma mass spectrometry (LA-MC-ICP-MS) at the University of Portsmouth, UK. The same 193 nm RESOlution Excimer laser used for U-Pb analyses was connected to a Nu Plasma I MC-ICP-MS. The following masses were measured in the respective Faraday collectors configuration: 171 (L_3), 173 (L_2), 175 (Ax), 176 (H_1), 177 (H_2), 178 (H_3), 179 (H_4) and 180 (H_5). Calibration of the equipment was realised utilizing raster lines on NIST 610 glass, Mud Tank and 91500 zircon standards. Laser conditions for tuning were 40 µm, 4.5 J/cm^2 and 5 Hz and total Hf intensity was typically 17 V for Mud Tank and 10 V for 91500. For the unknown analyses, only grains with a concordant U–Pb age and sufficient material remaining were analysed, using 50/60 µm spots on top of the U–Pb pits. Laser fluence was 4.0 J/cm^2, repetition rate was 6 Hz and gas flows were Ar 0.8 L/min and He 300 mL/min. The isotopes ^{171}Yb, ^{173}Yb and ^{175}Lu were monitored to allow for correction of isobaric interferences of Lu and Yb isotopes on mass 176. Reproducibility of the analyses was assured by periodic measurements of Plešovice (Sláma et al., 2008), 91500 (Blichert-Toft, 2008), Mud Tank (Woodhead and Hergt, 2005) and Temora 2 (Wu et al., 2006) and are consistent with published values. A number of analyses were carried out on top of previous U-Pb analyses in the standards and show no difference compared to analyses acquired on flat surface of the same materials. Data reduction was based on Hawkesworth and Kemp (2006). εHf values were calculated based on a two-stage model, using the bulk Earth (chondrite uniform reservoir; CHUR) $^{176}Hf/^{177}Hf$ and $^{176}Lu/^{177}Hf$ from Bouvier et al., (2008), depleted mantle (DM) $^{176}Hf/^{177}Hf$ and $^{176}Lu/^{177}Hf$ from Griffin et al., (2002), and the ^{176}Lu decay constant from Söderlund et al. (2004). Model ages were calculated assuming an average crustal $^{176}Lu/^{177}Hf$ value of 0.015 (Griffin et al., 2002).

It is important to note that unknown zircons are abundant in ^{176}Yb, having 30% to 50% of the total Yb. This mass bias was corrected and the errors propagated to the final data, which yielded less precise ratios when compared to the standards. Nonetheless, the ratios are consistent and εHf values tightly cluster between +6 and +10.

4. Metamorphic petrology

4.1. Sample description and petrology

Sample MD-16-01 (garnet-staurolite-sillimanite paragneiss) was also analysed in order to determine its metamorphic conditions.

Staurolite occurs in two different textures in the rock. Frequently it occurs as rounded inclusions within plagioclase and less commonly within garnet and anthophyllite. It is also found in quartz and plagioclase (up to 1-2 mm in size) dominated domains in the matrix where it occurs with sillimanite. If matrix staurolite is only in the presence of plagioclase, then it is occasionally replaced by symplectites of spinel.

The matrix foliation is defined by anthophyllite and biotite (up to 1.5 mm), although both of these can cross cut the foliation. Occasionally laths of sillimanite occur almost entirely within plagioclase grains (sometimes occurring with staurolite), these are always oriented parallel to the foliation. Garnet grains are anhedral and fragmented (fragments are up to 4 mm but groupings of fragments can be up to 1 cm in diameter). Some grains appear to have a core which is poikiloblastic (inclusions of quartz, plagioclase, rutile and occasionally staurolite and possibly kyanite). Other fragments are inclusion poor but occasionally preserve a fibrolite line which demarks a euhedral garnet, where inclusions occur they are sillimanite, staurolite, biotite and rutile.

Anthophyllite occurs as blades (up to 5 mm in length) and is variably replaced by biotite and chlorite, in some instances it is nearly pristine while in other places it is almost entirely replaced by chlorite. Anthophyllite is occasionally found as an inclusion in plagioclase and itself has inclusions of staurolite and rutile. Where anthophyllite is found with staurolite, the contact is marked by the growth of biotite and quartz.

Ilmenite and rutile are found in the matrix and as inclusions in garnet and anthophyllite.

4.2 Analytical methods

Pressure-temperature pseudosections were calculated for sample MD-16-01 using THERMOCALC V.3.33 (June 2009 update of Powell & Holland 1988) in the geologically realistic system MnNCKFMASHTO (MnO-Na_2O-CaO-K_2O-FeO-MgO-Al_2O_3-SiO_2-H_2O-TiO_2-Fe_2O_3) (Fig.8). Even though a revised thermodynamic dataset is now available (Holland and Powell 2011) and updated activity-composition (*a*-*x*) models (White et al 2014a,b), at the time the calculations for this study were conducted, the models were only calibrated for the Mn-free system, thus this study uses the dataset of (Holland and Powell 1998) and a-x models compatible with that dataset. The calculations included MnO because a small amount of MnO can have an important effect on stabilizing garnet to lower pressures than predicted in modelling with the MnO-free system (e.g. Mahar et al. 1997; White et al. 2014b). The modelling for this system uses the *a-x* relationships of White et al. (2007) for silicate melt; a combination of Mahar et al (1997) and Holland & Powell (1998) for cordierite and staurolite; White et al (2005) for garnet, biotite, ilmenite and hematite; White et al. (2002) for orthopyroxene, spinel and magnetite; a combination of Mahar et al (1997) and White et al (2000) for chloritoid; Coggon and Holland (2002) for muscovite and paragonite; Diener et al (2007) for orthoamphibole; Holland & Powell (1998) for epidote; a combination of Mahar et al (1997) and Holland et al (1998) for chlorite; and Holland & Powell (2003) for plagioclase and alkali feldspar.

The bulk composition of the sample was obtained by whole-rock X-ray fluorescence (XRF) analysis. For the lower temperature part of the diagram (<650°C), the H_2O content is set in excess. For the calculation of the solidus, H_2O was set such that the solidus was H_2O present for the entire diagram.

The proportion of Fe_2O_3 to FeO has been estimated considering the abundance of Fe^{3+}-bearing minerals. In addition, a T-$M$$Fe_2O_3$ diagram was calculated at 7.5 kbar. Compositional isopleths for garnet were calculated and have been plotted onto the peak field of the pseudosection to aid with interpretation of the *P-T* path.

4.3. Results

The peak assemblage is interpreted to be garnet + orthoamphibole + sillimanite + biotite + plagioclase + quartz + rutile, this occurs on the phase diagram at 625-700 °C and 6-7.5 kbars (Fig. 10). The *P-T* path can be defined by the change of mineral assemblage and the growth of garnet. Staurolite occurs as inclusions in garnet and preserved in the matrix (not in contact with quartz) and is inferred to have been stable during the prograde evolution of the sample. Ilmenite is also preserved within garnet. Together this gives an up-P and T evolution with peak conditions of 6-7 kbar and 650-700 °C. An inclusion of kyanite with staurolite in garnet potentially indicates that the P-T path may have pass through the kyanite bearing field before reaching peak conditions in the sillimanite bearing field. However, the complex zonation of garnet could indicate this sample has actually experienced multiple metamorphic events.

Garnet isopleths were calculated for the peak field. Compositions obtained from garnet with sillimanite inclusions (Burns 1994) are interpreted to have grown during peak metamorphic conditions and give compositions of ca. 0.57, 0.07 and 0.01 for X_{alm}, X_{grs} and X_{sps} respectively. This is broadly similar to values obtained from the model in the peak field (0.58-0.6 for X_{alm}, 0.1 to 0.02 for X_{sps} and 0.06 to 0.07 for X_{grs}). Unfortunately, the garnet compositions do not offer any additional constraints on the peak *P-T* conditions.

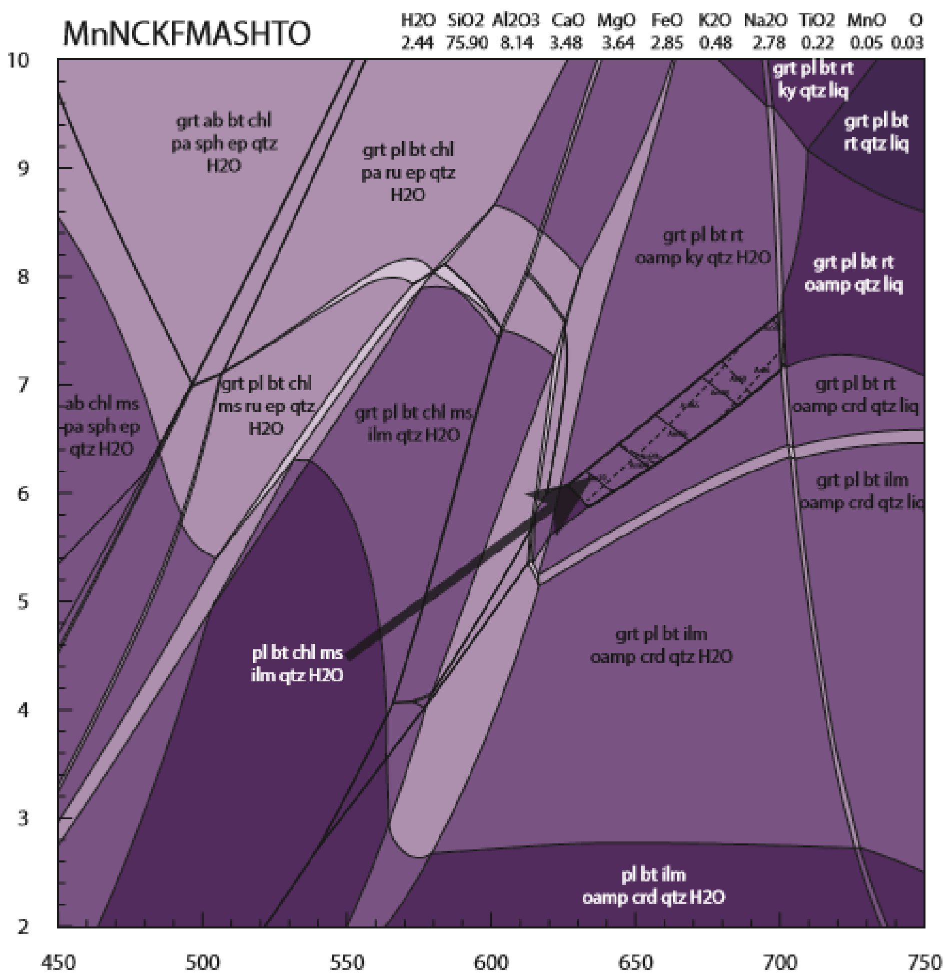

Fig. 10. Calculated phase diagram for sample MD-16-01. Mineral abbreviations from Kretz (1983) except orthoamphibole (Oamp). Left hand axis corresponds to pressures in kb, lower axis corresponds to temperature in degrees centigrade.

References

Axelsson, E., Pape, J., Berndt, J., Corfu, F., Mezger, K. and Raith, M. M., 2018. Rutile R632 - A new natural reference material for U-Pb and Zr determination. Geostandards and Geoanalytical Research, 42 (3), 319-338.

Black, L.P., Kamo, S.L., Allen, C.M., Aleinikoff, J.N., Davis, D.W., Korsch, R.J., and Foudoulis, C., 2003. TEMORA 1: a new zircon standard for Phanerozoic U-Pb geochronology. Chemical Geology, 200, 155-170. doi: 10.1016/S00009-2541(03)00165-7.

Blichert-Toft, J., 2008. The Hf isotopic composition of zircon reference material 91500: Chemical Geology, 253, 252–257.

Bouvier, A., Vervoort, J.D., and Patchett, P.J., 2008. The Lu–Hf and Sm–Nd isotopic composition of CHUR: constraints from unequilibrated chondrites and implications for the bulk composition of terrestrial planets: Earth and Planetary Science Letters, v. 273, 48–57.

Burns, I.M., 1994. Tectonothermal evolution and petrogenesis of the Naver and Kirtomy nappes, north Sutherland. PhD thesis, Oxford Brookes University.

Burns, I.M., Fowler, M.B., Strachan, R.A. and Greenwood, P.B., 2004. Geochemistry, petrogenesis and structural setting of the meta-igneous Strathy Complex: a unique basement block within the Scottish Caledonides? Geological Magazine, v. 141, p. 209-223.

Chew, D.M., Petrus, J.A. and Kamber, B.S., 2014. U–Pb LA–ICPMS dating using accessory mineral standards with variable common Pb. Chemical Geology, 363, 185-199.

Coggon, R., and Holland, T.J.B., 2002, Mixing properties of phengitic micas and revised garnet-phengite thermobarometers: Journal of Metamorphic Geology, v. 20, p. 683-696.

DePaolo, D.J., 1981. Neodymium isotopes in the Colorado Front Range and crust-mantle evolution in the Proterozoic. Nature, 291, 193-196.

DePaolo, D.J., Linn, A.M, and Schubert, G., 1991. The continental crustal age distribution: methods of determining mantle separation ages from Sm-Nd isotopic data and application to the southwestern United States. Journal of Geophysical Research, 96, 2071-2088.

Diener, J.F.A., Powell, R., White, R.W., and Holland, T.J.B., 2007, A new thermodynamic model for clino- and orthoamphiboles in the system Na_2O-CaO-FeO-MgO-Al_2O_3-SiO_2-H_2O-O: Journal of Metamorphic Geology, v. 25, p. 631-656.

Eugster, O., Tera, F., Burnett, D.S., and Wasserburg, G.J., 1970. Isotopic composition of gadolinium and neutron-capture effects in some meteorites. Journal of Geophysical Research, 75, 2753-2768.

Frei, D., Gerdes, A., 2009. Precise and accurate in-situ U-Pb dating of zircon with high sample throughput by automated LA-SF-ICP-MS, Chemical Geology, 26, 261-270.

Gehrels, G.E., Valencia, V. and Ruiz, J., 2009. Enhanced precision, accuracy, efficiency and special resolution of U-Pb ages by laser ablation-multicollector-inductively coupled plasma-mass spectrometry. Geochemistry Geophysics Geosystems, 9 (3).Gonçalves, G.O., Lana, C., Scholz, R., Buick, I.S., Gerdes, A., Kamo, S.L., Corfu, F., Marinho, M.M., and Chaves, A.O., 2016. An assessment of monazite from the Itambé pegmatite district for use as U-Pb isotope reference material for microanalysis and implications for the origin of the "Moacyr" monazite. Chemical Geology, 424, 30-50. doi: 10.1016/j.chemgeo.2015.12.019

Geisler, T., Pidgeon, R.T., van Bronswijk, W. and Kurtz, R., 2002. Transport of uranium, thorium, and lead in metamict zircon under low-temperature hydrothermal conditions. Chemical Geology, 191, 141-154. https://doi.org/10.1016/S0009-2541(02)00153-5

Goudie, D.J., Fisher, C.M., Hanchar, J.M., Crowley, J.L., and Ayers, J.C. 2014. Simultaneous in situ determination of U-Pb and Sm-Nd isotopes in monazite by laser ablation ICP-MS. Geochemistry, Geophysics, Geosystems, 15, 2575-2600. doi: 10.1002/2014GC005431

Griffin, W.L., Wang, X., Jackson, S.E., Pearson, N.J., O'Reilly, S.Y., Xu, X., and Zhou, X. 2002. Zircon chemistry and magma mixing, SE China: In situ analysis of Hf isotopes, Tonglu and Pingtan igneous complexes: Lithos, v. 61, 237-269.

Hawkesworth, C.J., and Kemp, A.I.S., 2006. Using hafnium and oxygen isotopes in zircons to unravel the record of crustal evolution: Chemical Geology, v. 226(3-4), 144-162.

Holland, T.J.B., and Powell, R., 1998, An internally consistent thermodynamic data set for phases of petrological interest: Journal of Metamorphic Geology, v. 16, p. 309-34.

Holland, T.J.B., and Powell, R., 2003, Activity-composition relations for phases in petrological calculations: an asymmetric multicomponent formulation: Contributions to Mineralogy and Petrology, v. 145, p. 492-501.

Horstwood, M.S., Foster, G.L., Parrish, R.R., Noble, S.R., and Nowell, G.M., 2003. Common-Pb corrected in situ: U-Pb accessory mineral geochronology by LA-MC-ICP-MS. The Royal Society of Chemistry, 18, 837-846. doi: 10.1039/b304365g

Jackson, S.E., Pearson, N.J., Griffin, W.L., and Belousova, E.A., 2004. The application of laser ablation-inductively coupled plasma mass spectrometry to in situ U-Pb zircon geochronology. Chemical Geology, 211, 47-69. doi: 10.1016/j.chemgeo.2004.06.017

Jacobsen, S.B. and Wasserburg, G.J., 1984. Sm-Nd isotopic evolution of chondrites and achondrites II. Earth and Planetary Science Letters, 67, 137-150.

Kretz, R., 1983, Symbols for rock-forming minerals: American Mineralogist, v. 68, p. 277-279.

Lana, C., Farina, F., Gerdes, A., Alkmim, A., Goncalves, G.O. and Jardim, A.C., 2017. Characterization of zircon reference materials via high precision U–Pb LA-MC-ICP-MS. Journal of Analytical Atom Spectrometry, 32(10), 2011-2023.

Ludwig, K.R., 1992. User's manual for ANALYST version 2.00; an IBM-PC computer program for control of a thermal-ionisation, single-collector mass-spectrometer. USGS Open File Report 92-0543.

Ludwig, K.R., 2003. User's Manual for Isoplot 3.00: a geochronological toolkit for Microsoft Excel (No. 4). Kenneth R. Ludwig.

Lugmair, G. and Marti, K., 1978. Lunar initial $^{143}Nd/^{144}Nd$: Differential evolution of the lunar crust and mantle. Earth and Planetary Science Letters, 35, 273-284.

Luvizotto, G.L., Zack, et al., 2009, Rutile crystals as potential trace element and isotope mineral standards for microanalysis: Chemical Geology, v. 261, p. 346-359.

Maclachlan, K., Rayner, N., Dunning, G., and Leugner, C., 2004. New results and ideas from the Rottenstone Domain project. Summary of Investigations, 2, 2004-4.

Mahar, E.M., Baker, J.M., Powell, R., Holland, T.J.B., and Howell, N., 1997, The effect of Mn on mineral stability in metapelites: Journal of Metamorphic Geology, v. 15, p. 223-238.

Miller, J.S., Matzel., J.E.P., Miller, C.F., Burgess, S.D. and Miller, R.B., 2007. Zircon growth and recycling during the assembly of large, composite arc plutons. Journal of Volcanology and Geothermal Research, 167, 282-299.

Paton, C., Hellstrom, J., Paul, B., Woodhead, J., and Hergt, J., 2011. Iolite: Freeware for the visualisation and processing of mass spectrometric data. Journal of Analytical Atomic Spectrometry, 26, 2508. doi: 10.1039/c1ja10172b

Santos, M., Lana, C., Scholz, R., Buick, I., Schmitz, M.D., Kamo, S.L., Gerdes, A., Corfu, F., Tapster, S., Lancaster, P., Storey, C.D., Basei, M.A.S., Tohver, E., Alkmim, A., Nadini, H., Krambrock, K., Fantini, C., and Wiedenbeck, M., 2017. A New Appraisal of Sri Lankan BB Zircon as a Reference Material for LA-ICP-MS U-Pb Geochronology and Lu-Hf Isotope Tracing. Geostandards and Geoanalytical Research, v. 41. p. 335-358. doi: 10.1111/ggr.12167

Seydoux-Guillaume, A-M., Bingen, B., Paquette, J-L. and Bosse, V., 2015. Nanoscale evidence for uranium mobility in zircon and the discordance of U–Pb chronometers. Earth and Planetary Science Letters, 409, 43-48. https://doi.org/10.1016/j.epsl.2014.10.044

Sláma, J., Kossler, J., et al., 2008. Plešovice zircon – A new natural reference material for U-Pb and Hf isotopic microanalysis. Chemical Geology, 249, 1-35. doi: 10.1007/PL00007673

Söderlund, U., Patchett, J.P., Vervoort, J.D., Isachsen, C.E., 2004. The 176Lu decay constant determined by Lu-Hf and U-Pb isotope systematics of Precambrian mafic intrusions: Earth and Planetary Science Letters, v. 219, 311-324.

Tomascak, P.B., Krogstad, E.J., and Walker, R.J., 1996. U-Pb monazite geochronology of granitic rocks from Maine: Implications for Late Palaeozoic tectonics in the Northern Appalachians. Journal of Geology, 104, 185-195. doi: 10.2307/256788.

White, R.W., Powell, R., Holland, T.J.B. & Worley, B.A., 2000. The effect of TiO2 and Fe2O3 on metapelite assemblages at greenschist and amphibolites facies conditions: mineral equilibria calculations in the system K2O-FeO-MgO-Al2O3-SiO2-H2O-TiO2-Fe2O3. Journal of Metamorphic Geology, 18, 497–511.

White, R.W., Powell, R., and Clarke, G.L., 2002, The interpretation of reaction textures in Fe-rich metapelitic granulites of the Musgrave Block, central Australia: Constraints from mineral equilibria calculations in the system K_2O-FeO-MgO-Al_2O_3-SiO_2-H_2O-TiO_2-Fe_2O_3: Journal of Metamorphic Geology, v. 20, p. 41-55.

White, R.W., Pomroy, N.E., and Powell, R., 2005. An in situ metatexite-diatexite transition in upper amphibolite facies rocks from Broken Hill, Australia: Journal of Metamorphic Geology, v. 23, p. 579-602.

White, R.W., Powell, R. & Holland, T.J.B., 2007. Progress relating to calculation of partial melting equilibria for metapelites. Journal of Metamorphic Geology, 25, 511–527.

White, R.W., Powell, R., Holland, T.J.B., Johnson, T.E. & Green, E.C.R., 2014a. New mineral activity–composition relations for thermodynamic calculations in metapelitic systems. Journal of Metamorphic Geology, 32, 261–286.

White, R.W., Powell, R. & Johnson, T.E., 2014b. The effect of Mn on mineral stability in metapelites revisited: new a–x relations for manganese-bearing minerals. Journal of Metamorphic Geology, 32, 809–828.

Wiedenbeck, M., Allé, P., et al., 1995. Three natural zircon standards for U-Th-Pb, Lu-Hf, trace element and REE analyses. Geostandards and Geoanalytical Research, 19, 1-23. doi: 10.1111/j.1751-908X.1995.tb00147.x

Woodhead, J.D., and Hergt, J.M., 2005. A preliminary appraisal of seven natural zircon reference materials for in situ Hf isotope determination: Geostandards and Geoanalytical Research, v. 29(2), 183-195.

Wu, F.-Y., Yang, Y.-H., Xie, L.-W., Yang, J.-H., Xu, P., 2006. Hf isotopic compositions of the standard zircons and baddeleyites in U–Pb geochronology: Chemical Geology, v. 234, 105–126.

Zack, T., Stockli, D.F., Luvizotto, G.L., Barth, M.G., Belousova, E. and Wolfe, M.R., 2011. In situ U–Pb rutile dating by LA-ICP-MS: ^{208}Pb correction and prospects for geological applications, Contributions to Mineralogy and Petrology, v. 162, p. 515-530.

Table DR4

Zircon Samples

Sample	Spot size (µm)	U (ppm)	$^{206}Pb^{a}/^{238}U$	±2s	$^{207}Pb^{a}/^{235}U$	±2s	Rho[c]	Th/U	$^{207}Pb/^{206}Pb$	±2s (Ma)	$^{206}Pb/^{238}U$	±2s (Ma)	$^{207}Pb/^{235}U$	±2s (Ma)	Conc.[d]
RS-14-16															
16-Z23-b	11	3401	0.0611	0.0008	0.462	0.009	0.501	0.01	446	40	382	5	384	6	99.4
16-Z08	11	699	0.0679	0.0014	0.526	0.021	0.147	0.02	421	85	424	9	428	14	99.0
16-Z28	11	1382	0.0688	0.0015	0.540	0.016	0.248	0.03	459	58	429	9	438	11	97.9
16-Z24	11	2079	0.0691	0.0015	0.519	0.023	0.231	0.05	354	94	431	9	423	15	101.8
16-Z23	11	3000	0.0702	0.0011	0.538	0.009	0.198	0.00	432	37	438	6	437	6	100.1
16-Z14	11	1256	0.0721	0.0016	0.559	0.022	0.147	0.10	423	84	449	9	450	14	99.7
16-Z09	9	1141	0.0728	0.0007	0.562	0.017	0.140	0.04	417	60	453	4	451	11	100.5
16-Z07	9	1220	0.0741	0.0007	0.579	0.018	0.209	0.05	442	61	461	4	462	11	99.7
16-Z12	9	834	0.0742	0.0008	0.577	0.019	0.140	0.01	425	68	461	5	461	12	100.0
16-Z45	9	973	0.0747	0.0016	0.586	0.034	0.103	0.12	460	110	464	9	465	22	99.8
16-Z48	9	877	0.0752	0.0016	0.588	0.026	0.327	0.57	449	77	467	9	468	17	99.8
16-Z04	11	1082	0.0786	0.0013	0.629	0.021	0.014	0.66	518	76	488	8	498	13	97.9
16-Z42	9	1562	0.0798	0.0014	0.627	0.024	0.217	0.83	479	64	495	8	493	15	100.3
16-Z21	11	1451	0.0807	0.0016	0.632	0.016	0.128	0.90	465	46	500	10	496	10	100.8
16-Z11	9	601	0.0807	0.0009	0.648	0.024	0.055	0.41	518	74	500	6	507	14	98.6
16-Z26	11	768	0.0807	0.0009	0.635	0.018	0.026	0.63	479	65	500	6	497	11	100.7
16-Z29	11	1493	0.0810	0.0017	0.641	0.018	0.073	0.82	483	56	502	10	503	11	99.8
16-Z52	11	695	0.0810	0.0008	0.634	0.018	0.255	0.47	498	59	502	5	496	11	101.2
16-Z53	9	644	0.0812	0.0013	0.648	0.022	0.130	0.48	484	68	503	8	505	13	99.6
16-Z39	11	674	0.0813	0.0018	0.638	0.035	0.252	0.31	490	120	504	11	497	22	101.4
16-Z17	11	1726	0.0814	0.0017	0.640	0.018	0.215	0.62	455	56	505	10	501	11	100.7
16-Z15	11	934	0.0819	0.0008	0.646	0.017	0.171	0.56	482	57	507	5	505	10	100.5
16-Z62	9	1089	0.0822	0.0013	0.659	0.022	0.065	0.57	501	71	509	8	512	13	99.4
16-Z05	9	1177	0.0832	0.0013	0.638	0.031	0.058	0.42	424	100	515	8	498	19	103.3
16-Z48-b	9	1115	0.0842	0.0014	0.674	0.022	0.278	0.55	519	64	521	8	521	13	100.0
16-Z57	9	700	0.0848	0.0014	0.658	0.022	0.124	0.46	419	70	525	9	510	14	102.8
MD-16-05															
05-Z01-C	9	561	0.0743	0.0017	0.553	0.041	0.223	0.11	340	150	462	10	441	27	104.5
05-Z02-R	9	1028	0.0631	0.0013	0.476	0.030	0.164	0.09	390	130	394	8	393	20	100.4
05-Z03-R	9	2990	0.0714	0.0008	0.537	0.017	0.317	0.02	388	62	444	5	435	11	102.0
05-Z04-R	9	1501	0.0699	0.0007	0.542	0.016	0.141	0.21	427	60	436	4	438	10	99.5
05-Z05-R	11	2097	0.0704	0.0014	0.529	0.013	0.207	0.22	379	46	438	8	431	8	101.8
05-Z06-C	11	2352	0.0699	0.0016	0.522	0.019	0.179	0.08	347	74	436	9	425	13	102.5
05-Z11-R	11	593	0.0756	0.0019	0.586	0.035	0.183	0.10	370	120	470	12	463	23	101.5
05-Z21-C	9	896	0.0705	0.0017	0.539	0.029	0.188	0.16	389	100	439	10	436	19	100.8
05-Z24-R	9	938	0.0678	0.0018	0.514	0.033	0.261	0.06	380	120	423	11	419	22	100.9
05-Z30-C	9	831	0.0678	0.0016	0.508	0.028	0.238	0.29	355	100	423	10	417	18	101.4
MD-16-06															
06-Z01-R	9	258	0.0678	0.0013	0.537	0.032	0.095	0.17	410	120	423	8	430	22	98.3
06-Z02-C	9	4218	0.0716	0.0006	0.555	0.013	0.311	0.32	447	47	446	4	448	9	99.5
06-Z03-R	9	2553	0.0708	0.0006	0.542	0.013	0.316	0.56	405	49	441	3	439	9	100.5
06-Z04-R	11	634	0.0691	0.0018	0.545	0.029	0.125	0.06	440	110	431	11	437	19	98.5
06-Z06-R	11	617	0.0761	0.0020	0.574	0.026	0.306	0.06	374	95	473	12	457	17	103.3
06-Z07-C	11	628	0.0720	0.0015	0.562	0.020	0.016	0.27	432	74	448	9	451	13	99.3
06-Z08-R	11	340	0.0669	0.0017	0.519	0.026	0.062	0.16	390	100	417	10	418	18	99.8
06-Z09-R	11	1445	0.0699	0.0014	0.541	0.016	0.229	0.28	406	57	435	9	439	11	99.2
06-Z10-C	11	1027	0.0676	0.0014	0.536	0.016	0.056	0.33	451	58	422	8	434	10	97.0
06-Z10-R	11	1409	0.0676	0.0014	0.531	0.015	0.223	0.27	432	53	422	8	431	10	97.7
06-Z14-C	9	872	0.0661	0.0013	0.508	0.024	0.006	0.59	393	89	413	8	415	16	99.4
06-Z23-R	9	4340	0.0732	0.0013	0.553	0.021	0.472	0.59	390	58	455	8	446	14	102.0
06-Z46-C	9	1082	0.0700	0.0012	0.526	0.023	0.211	0.47	371	74	436	7	429	16	101.6
MD-16-07															
07-Z01-C	9	268	0.0678	0.0012	0.532	0.034	0.127	0.21	380	120	423	7	422	23	100.1
07-Z02-C	9	363	0.0668	0.0016	0.512	0.039	0.140	0.16	380	150	416	10	413	26	100.8
07-Z03-R	9	1154	0.0655	0.0011	0.515	0.024	0.099	0.31	461	99	409	7	419	16	97.6
07-Z04-C	9	2660	0.0744	0.0009	0.592	0.017	0.347	0.19	487	56	463	5	471	11	98.3
07-Z04-R	9	2456	0.0673	0.0007	0.518	0.015	0.322	0.51	412	58	420	4	423	10	99.4
07-Z05-C	11	873	0.0677	0.0017	0.540	0.031	0.082	0.35	480	120	422	10	435	20	96.9
07-Z05-R	11	363.8	0.0671	0.0018	0.535	0.032	0.152	0.08	450	120	418	11	429	21	97.5
07-Z06-R	11	1212	0.0663	0.0015	0.529	0.020	0.146	0.32	497	81	414	9	429	14	96.3
07-Z07-C	11	504	0.0675	0.0016	0.517	0.025	0.070	0.43	395	96	421	10	419	17	100.5
07-Z15-C	9	1840	0.0720	0.0013	0.549	0.023	0.254	0.39	412	70	448	8	443	15	101.2
07-Z17-C	9	899	0.0688	0.0016	0.502	0.032	0.084	0.28	330	130	429	10	414	23	103.5
07-Z28-C	9	649	0.0697	0.0012	0.535	0.023	0.090	0.26	400	73	435	8	433	15	100.5
07-Z31-R	9	527	0.0726	0.0019	0.527	0.036	0.017	0.21	280	130	452	11	425	24	105.9
07-Z20-C	9	1382	0.0728	0.0015	0.569	0.023	0.376	0.21	475	80	453	9	458	15	98.8
07-Z38-C	9	897	0.0706	0.0013	0.552	0.022	0.085	0.30	476	88	440	8	444	14	99.1
07-Z42-C	9	1050	0.0709	0.0016	0.558	0.027	0.124	0.28	490	100	441	10	448	17	98.5
07-Z68-C	9	848	0.0735	0.0017	0.599	0.032	0.111	0.23	550	120	457	10	474	21	96.3

acorrected for background, instrumental drift and mass bias fractionation based on primary stantard.

c rho is the 207Pb/235U/206Pb/238U error correlation coefficient.

d degree of concordance: 100-((1+((206Pb/238U - 207Pb/235U)/206Pb/238U)) x 100)

Zircon Standards

Sample	Spot size (µm)	U (ppm)	$^{206}Pb^{a}/^{238}U$	±2s	$^{207}Pb^{a}/^{235}U$	±2s	Rho[c]	Th/U	$^{207}Pb/^{206}Pb$	±2s (Ma)	$^{206}Pb/^{238}U$	±2s (Ma)	$^{207}Pb/^{235}U$	±2s (Ma)	Conc.[d]
Primary															
Plesovice1	11	756	0.0538	0.0012	0.391	0.015	0.144	0.04	284	68	338	7	333	11	100.5
Plesovice2	11	752	0.0539	0.0012	0.400	0.016	0.192	0.04	328	70	338	7	340	12	98.4
Plesovice3	11	756	0.0539	0.0012	0.396	0.015	0.107	0.04	307	70	338	7	337	11	99.5
Plesovice4	11	751	0.0538	0.0012	0.393	0.015	0.185	0.04	293	66	338	7	335	11	99.9
Plesovice5	11	766	0.0534	0.0012	0.393	0.016	0.165	0.04	297	72	335	7	334	12	99.4
Plesovice6	11	756	0.0536	0.0012	0.387	0.015	0.109	0.04	282	71	337	7	330	11	101.0
Plesovice7	11	756	0.0542	0.0012	0.404	0.017	0.114	0.04	321	74	340	7	342	12	98.4
Plesovice8	11	767	0.0529	0.0012	0.389	0.016	0.120	0.04	292	71	332	7	331	11	99.3
Plesovice9	11	745	0.0537	0.0012	0.395	0.015	0.086	0.04	312	70	337	7	337	11	99.1
Plesovice10	11	752	0.0534	0.0012	0.391	0.016	0.050	0.04	284	73	335	7	333	12	99.7
Plesovice11	11	755	0.0540	0.0012	0.399	0.016	0.077	0.04	312	72	339	7	338	11	99.2
Plesovice12	11	739	0.0541	0.0012	0.398	0.017	0.065	0.04	306	77	340	7	337	12	99.8
Plesovice13	11	757	0.0533	0.0011	0.386	0.016	0.098	0.04	274	73	335	7	329	12	100.7
Plesovice14	11	758	0.0547	0.0012	0.405	0.016	0.028	0.04	329	73	343	7	344	12	98.7
Plesovice15	11	755	0.0533	0.0011	0.388	0.015	0.071	0.04	291	69	335	7	331	11	100.1
Plesovice16	11	765	0.0538	0.0007	0.396	0.018	0.048	0.05	265	88	338	4	335	13	99.7
Plesovice17	11	807	0.0536	0.0007	0.389	0.018	0.135	0.05	257	92	336	4	330	13	100.9
Plesovice18	11	744	0.0537	0.0008	0.396	0.018	0.083	0.05	272	88	337	5	335	13	99.7
Plesovice19	11	749	0.0536	0.0008	0.396	0.020	0.090	0.05	277	96	336	5	335	14	99.4
Plesovice20	11	740	0.0538	0.0008	0.395	0.020	0.081	0.05	252	98	338	5	334	15	100.1
Plesovice21	11	752	0.0537	0.0008	0.390	0.019	0.015	0.05	253	99	337	5	332	14	100.4
Plesovice22	11	755	0.0537	0.0009	0.396	0.020	0.132	0.05	266	95	337	5	335	14	99.6
Plesovice23	11	775	0.0536	0.0008	0.395	0.019	0.136	0.05	267	93	337	5	334	14	99.8
Plesovice24	11	744	0.0537	0.0008	0.394	0.020	0.030	0.05	230	100	337	5	332	15	100.5
Plesovice25	11	737	0.0538	0.0008	0.394	0.019	0.004	0.05	252	94	337	5	336	14	99.4
Plesovice26	11	749	0.0535	0.0008	0.393	0.019	0.053	0.05	258	98	336	5	334	14	99.6
Plesovice27	11	773	0.0537	0.0007	0.397	0.020	0.042	0.05	273	97	337	4	337	15	99.1
Plesovice28	11	755	0.0537	0.0007	0.389	0.019	0.017	0.05	238	97	337	5	331	14	100.9
Plesovice29	11	748	0.0537	0.0008	0.398	0.019	0.141	0.05	276	89	337	5	338	14	98.7
Plesovice30	11	758	0.0535	0.0009	0.392	0.020	0.149	0.05	256	96	336	5	333	14	99.9
Plesovice31	11	773	0.0538	0.0007	0.393	0.021	0.110	0.05	230	100	338	4	331	15	101.0
Plesovice32	11	747	0.0537	0.0008	0.395	0.021	0.130	0.05	268	99	337	5	335	15	99.6
Plesovice33	11	753	0.0536	0.0009	0.393	0.013	0.190	0.03	308	69	336	6	335	10	99.3
Plesovice34	11	788	0.0538	0.0009	0.396	0.013	0.051	0.03	317	70	338	6	337	9	99.1
Plesovice35	11	740	0.0539	0.0010	0.394	0.014	0.125	0.04	302	72	338	6	335	10	100.0
Plesovice36	11	744	0.0529	0.0009	0.392	0.015	0.043	0.04	301	79	332	6	333	11	98.8
Plesovice37	11	760	0.0545	0.0009	0.396	0.014	0.042	0.04	300	78	342	6	336	10	100.7
Plesovice38	11	755	0.0536	0.0010	0.393	0.016	0.115	0.04	295	81	337	6	334	12	99.7
Plesovice39	11	757	0.0537	0.0010	0.393	0.014	0.165	0.04	293	74	337	6	335	10	99.5
Plesovice40	11	752	0.0538	0.0009	0.397	0.015	0.082	0.04	307	75	338	6	337	11	99.1
Plesovice41	11	756	0.0536	0.0009	0.393	0.015	0.085	0.04	294	78	337	6	336	11	99.2
Plesovice42	11	754	0.0534	0.0010	0.392	0.014	0.073	0.04	298	74	335	6	335	10	99.0
Plesovice43	11	757	0.0538	0.0010	0.396	0.014	0.204	0.04	308	72	338	6	337	10	99.2
Plesovice44	11	754	0.0537	0.0009	0.393	0.014	0.018	0.04	295	76	337	6	335	11	99.7
Plesovice45	11	755	0.0539	0.0008	0.388	0.020	0.116	0.05	287	130	339	5	331	14	101.2
Plesovice46	9	763	0.0535	0.0008	0.397	0.021	0.090	0.05	338	130	336	5	338	15	98.5
Plesovice47	9	751	0.0541	0.0008	0.388	0.020	0.119	0.05	256	130	340	5	331	15	101.7
Plesovice48	9	751	0.0539	0.0008	0.384	0.021	0.149	0.05	224	130	339	5	327	15	102.3
Plesovice49	9	752	0.0538	0.0009	0.411	0.021	0.245	0.05	363	130	338	5	348	15	96.0
Plesovice50	9	759	0.0532	0.0008	0.397	0.021	0.082	0.05	306	130	334	5	338	15	97.7
Plesovice51	9	755	0.0538	0.0008	0.391	0.021	0.102	0.05	233	130	338	5	332	15	100.6
Plesovice52	9	753	0.0534	0.0008	0.394	0.021	0.206	0.05	275	130	336	5	336	15	98.9
Plesovice53	9	757	0.0533	0.0008	0.406	0.021	0.182	0.05	332	130	335	5	345	16	96.0
Plesovice54	9	753	0.0536	0.0008	0.401	0.022	0.020	0.05	297	130	336	5	339	16	98.2
Plesovice55	9	757	0.0530	0.0008	0.391	0.021	0.169	0.05	294	130	333	5	333	15	98.8
Plesovice56	9	756	0.0543	0.0008	0.388	0.021	0.021	0.05	236	130	341	5	331	15	101.8
Plesovice57	9	752	0.0534	0.0008	0.394	0.020	0.148	0.05	313	130	335	5	336	15	98.9
Plesovice58	9	755	0.0538	0.0008	0.379	0.021	0.147	0.06	217	130	338	5	325	15	102.8
Plesovice59	9	757	0.0537	0.0008	0.393	0.020	0.121	0.05	298	130	337	5	335	15	99.8
Plesovice60	9	758	0.0541	0.0008	0.403	0.021	0.251	0.05	332	130	340	5	342	15	98.4
Plesovice61	9	751	0.0536	0.0006	0.385	0.015	0.194	0.04	261	76	337	4	328	11	101.6
Plesovice62	9	750	0.0538	0.0006	0.399	0.016	0.025	0.04	326	83	338	4	339	12	98.7
Plesovice63	9	760	0.0537	0.0007	0.392	0.014	0.076	0.04	292	71	337	4	334	10	100.0
Plesovice64	9	758	0.0541	0.0006	0.404	0.015	0.071	0.04	342	75	340	4	343	11	97.9
Plesovice65	9	751	0.0534	0.0006	0.396	0.015	0.101	0.04	328	75	336	4	339	11	98.0
Plesovice66	9	756	0.0535	0.0006	0.387	0.016	0.086	0.04	266	80	336	4	329	12	101.1
Plesovice67	9	751	0.0536	0.0006	0.404	0.016	0.042	0.04	349	82	337	4	342	12	97.4
Plesovice68	9	756	0.0539	0.0006	0.386	0.015	0.188	0.04	254	78	338	4	330	12	101.4
Plesovice69	9	758	0.0535	0.0006	0.390	0.015	0.113	0.04	279	75	336	4	332	11	100.3
Plesovice70	9	760	0.0537	0.0007	0.399	0.016	0.079	0.04	335	81	337	4	340	12	98.2
Plesovice71	9	751	0.0533	0.0006	0.396	0.016	0.104	0.04	311	78	335	4	337	11	98.3
Plesovice72	9	753	0.0535	0.0007	0.386	0.016	0.040	0.04	268	85	336	4	330	12	100.7
Plesovice73	9	752	0.0539	0.0006	0.405	0.018	0.009	0.04	342	89	339	4	342	13	98.0
Plesovice74	9	755	0.0536	0.0006	0.389	0.015	0.053	0.04	284	78	337	4	331	11	100.6
Plesovice75	9	762	0.0537	0.0007	0.397	0.015	0.112	0.04	312	74	337	4	337	11	99.0
Plesovice76	9	748	0.0536	0.0006	0.398	0.016	0.165	0.04	314	80	336	4	339	12	98.2
Plesovice77	9	759	0.0540	0.0006	0.403	0.015	0.011	0.04	344	76	339	4	344	11	97.6

Plesovice78	9	770	0.0537	0.0007	0.379	0.016	0.077	0.04	233	83	337	4	324	12	102.9
Plesovice79	9	741	0.0537	0.0012	0.390	0.015	0.086	0.04	285	74	337	7	333	11	100.3
Plesovice80	11	764	0.0538	0.0011	0.400	0.015	0.137	0.04	330	75	338	7	341	11	98.0
Plesovice81	11	750	0.0532	0.0012	0.382	0.015	0.043	0.04	247	78	334	7	326	11	101.5
Plesovice82	11	753	0.0541	0.0012	0.403	0.015	0.043	0.04	315	72	340	7	342	11	98.4
Plesovice83	11	750	0.0537	0.0011	0.400	0.016	0.064	0.04	327	78	337	7	340	11	98.2
Plesovice84	11	764	0.0538	0.0012	0.395	0.016	0.081	0.04	304	77	338	7	336	11	99.6
Plesovice85	11	742	0.0533	0.0011	0.388	0.015	0.236	0.04	296	71	335	7	331	11	100.2
Plesovice86	11	767	0.0536	0.0012	0.388	0.015	0.219	0.04	278	74	337	7	330	11	101.0
Plesovice87	11	763	0.0546	0.0012	0.403	0.015	0.073	0.04	328	76	343	7	342	11	99.2
Plesovice88	11	752	0.0532	0.0011	0.386	0.015	0.098	0.04	282	76	334	7	329	11	100.4
Plesovice89	11	751	0.0535	0.0011	0.402	0.016	0.006	0.04	353	77	336	7	340	11	97.8
Plesovice90	11	745	0.0540	0.0012	0.394	0.015	0.083	0.04	302	75	339	7	335	11	100.1
Plesovice91	11	759	0.0539	0.0011	0.395	0.015	0.042	0.04	291	72	339	7	336	11	99.8
Plesovice92	11	758	0.0536	0.0011	0.391	0.016	0.142	0.04	294	76	336	7	333	11	100.0
Plesovice93	11	751	0.0532	0.0011	0.393	0.015	0.220	0.04	334	70	334	7	335	11	98.6
Plesovice94	11	772	0.0538	0.0012	0.411	0.016	0.181	0.04	391	74	338	7	347	11	96.3
Plesovice95	11	754	0.0542	0.0012	0.403	0.016	0.030	0.04	336	80	340	7	341	12	98.8
Plesovice96	11	736	0.0534	0.0011	0.378	0.013	0.117	0.03	237	67	335	7	324	10	102.5
Plesovice97	11	768	0.0540	0.0012	0.398	0.016	0.168	0.04	314	74	339	7	338	11	99.4
Plesovice98	11	754	0.0533	0.0011	0.393	0.015	0.068	0.04	327	74	335	7	336	11	98.7
Plesovice99	11	754	0.0539	0.0011	0.394	0.015	0.039	0.04	283	76	338	7	335	11	99.9
Plesovice100	11	758	0.0539	0.0012	0.400	0.016	0.187	0.04	322	75	338	7	339	11	98.7
Plesovice101	11	754	0.0536	0.0012	0.397	0.015	0.029	0.04	323	72	337	7	337	11	98.9
Plesovice102	11	749	0.0536	0.0011	0.396	0.015	0.184	0.04	330	72	337	7	337	11	99.0
Plesovice103	11	746	0.0538	0.0011	0.386	0.014	0.100	0.04	288	68	338	7	331	10	101.2
Plesovice104	11	768	0.0534	0.0011	0.386	0.015	0.188	0.04	294	75	335	7	333	11	99.9
Plesovice105	11	762	0.0534	0.0012	0.383	0.015	0.122	0.04	260	77	336	7	327	11	101.5
Plesovice106	11	759	0.0539	0.0011	0.394	0.016	0.074	0.04	274	79	338	7	335	11	99.9
Plesovice107	11	742	0.0538	0.0011	0.394	0.015	0.034	0.04	270	77	338	7	336	11	99.6
Plesovice108	11	766	0.0542	0.0012	0.389	0.015	0.109	0.04	246	77	340	7	335	11	100.5
Plesovice109	11	752	0.0531	0.0011	0.396	0.016	0.026	0.04	322	81	333	7	336	12	98.2
Plesovice110	11	746	0.0536	0.0012	0.388	0.016	0.017	0.04	272	80	337	7	330	12	101.0
Plesovice111	11	753	0.0540	0.0012	0.391	0.016	0.109	0.04	270	79	339	7	332	12	101.0
Plesovice112	11	750	0.0537	0.0012	0.416	0.015	0.143	0.04	411	72	337	7	351	11	94.9
Plesovice113	11	767	0.0545	0.0009	0.392	0.016	0.158	0.04	257	85	342	5	334	12	101.3
Plesovice114	9	750	0.0535	0.0009	0.405	0.015	0.118	0.04	356	81	336	5	343	11	97.0
Plesovice115	9	758	0.0537	0.0009	0.385	0.016	0.032	0.04	255	89	337	5	329	12	101.5
Plesovice116	9	758	0.0536	0.0009	0.401	0.016	0.130	0.04	332	84	337	6	341	11	97.7
Plesovice117	9	752	0.0533	0.0009	0.388	0.015	0.100	0.04	294	83	334	5	330	11	100.3
Plesovice118	9	753	0.0536	0.0009	0.389	0.016	0.222	0.04	277	82	337	5	332	11	100.4
Plesovice119	9	766	0.0534	0.0009	0.391	0.015	0.043	0.04	295	80	335	5	333	11	99.7
Plesovice120	9	746	0.0533	0.0009	0.399	0.015	0.195	0.04	347	79	335	5	340	11	97.5
Plesovice121	9	761	0.0536	0.0009	0.386	0.014	0.014	0.04	270	81	337	5	329	10	101.2
Plesovice122	9	754	0.0539	0.0009	0.399	0.015	0.125	0.04	317	82	338	5	338	11	99.0
Plesovice123	9	753	0.0535	0.0009	0.402	0.016	0.075	0.04	343	87	336	5	341	12	97.5
Plesovice124	9	752	0.0543	0.0009	0.394	0.016	0.165	0.04	280	84	341	6	335	12	100.6
Plesovice125	9	756	0.0532	0.0008	0.389	0.016	0.156	0.04	280	86	334	5	331	12	99.9
Plesovice126	9	756	0.0537	0.0009	0.396	0.016	0.190	0.04	302	84	337	5	337	12	99.0
Plesovice127	9	750	0.0545	0.0008	0.390	0.016	0.039	0.04	240	86	342	5	332	12	101.9
Plesovice128	9	763	0.0534	0.0009	0.396	0.014	0.027	0.04	328	79	335	5	337	10	98.6
Plesovice129	9	753	0.0548	0.0010	0.403	0.019	0.112	0.05	301	76	344	6	341	13	99.6
Plesovice130	9	813	0.0535	0.0009	0.393	0.019	0.128	0.05	303	81	336	6	334	14	99.5
Plesovice131	9	749	0.0528	0.0010	0.383	0.018	0.095	0.05	275	77	332	6	327	13	100.4
Plesovice132	9	752	0.0537	0.0010	0.397	0.019	0.025	0.05	309	79	337	6	337	13	99.0
Plesovice133	9	742	0.0539	0.0010	0.403	0.018	0.117	0.04	343	74	338	6	342	13	97.8
Plesovice134	9	771	0.0539	0.0010	0.395	0.017	0.030	0.04	311	75	339	6	336	13	99.7
Plesovice135	9	750	0.0534	0.0010	0.383	0.017	0.100	0.04	259	76	335	6	327	13	101.4
Plesovice136	9	760	0.0540	0.0010	0.403	0.018	0.082	0.04	356	74	339	6	344	13	97.6
Plesovice137	9	743	0.0540	0.0009	0.393	0.018	0.026	0.05	283	79	339	6	334	13	100.5
Plesovice138	9	743	0.0530	0.0010	0.383	0.018	0.061	0.05	279	81	333	6	327	13	100.7
Plesovice139	9	748	0.0533	0.0010	0.385	0.018	0.088	0.05	282	79	334	6	329	13	100.8
Plesovice140	9	749	0.0541	0.0010	0.398	0.018	0.007	0.05	312	75	339	6	338	13	99.4
Plesovice141	9	737	0.0528	0.0010	0.396	0.019	0.091	0.05	334	82	332	6	336	14	97.8
Plesovice142	9	763	0.0535	0.0010	0.392	0.018	0.082	0.05	301	77	336	6	334	13	99.6
Plesovice143	9	762	0.0537	0.0010	0.412	0.019	0.162	0.05	392	78	337	6	348	14	95.7
Plesovice144	9	770	0.0545	0.0010	0.401	0.018	0.093	0.04	316	77	342	6	341	13	99.4
Plesovice145	9	725	0.0536	0.0009	0.387	0.018	0.133	0.05	278	77	337	6	331	13	100.7
Plesovice146	9	775	0.0535	0.0010	0.390	0.018	0.044	0.05	291	77	336	6	332	13	100.0
Plesovice147	9	761	0.0541	0.0010	0.391	0.018	0.025	0.05	286	80	340	6	334	13	100.6
Plesovice148	9	760	0.0538	0.0010	0.393	0.018	0.193	0.05	298	74	338	6	335	13	99.7
Plesovice149	9	758	0.0535	0.0008	0.393	0.015	0.122	0.04	291	74	336	5	336	11	98.8
Plesovice150	9	755	0.0541	0.0009	0.401	0.014	0.188	0.03	333	73	339	5	342	11	98.4
Plesovice151	9	756	0.0536	0.0008	0.389	0.014	0.067	0.04	283	74	336	5	331	11	100.5
Plesovice152	9	752	0.0537	0.0009	0.391	0.015	0.163	0.04	297	75	337	5	332	11	100.5
Plesovice153	9	757	0.0537	0.0008	0.396	0.015	0.085	0.04	333	78	337	5	336	11	99.3
Plesovice154	9	756	0.0537	0.0008	0.403	0.015	0.132	0.04	355	75	337	5	341	11	97.9
Plesovice155	9	753	0.0537	0.0008	0.386	0.015	0.003	0.04	281	76	337	5	330	10	101.2
Plesovice156	9	758	0.0536	0.0008	0.383	0.014	0.171	0.04	258	70	336	5	328	10	101.5
Plesovice157	9	754	0.0537	0.0008	0.403	0.013	0.077	0.03	356	67	337	5	342	10	97.5
Plesovice158	9	756	0.0538	0.0008	0.395	0.015	0.241	0.04	292	74	338	5	336	11	99.5
Plesovice159	9	753	0.0536	0.0008	0.386	0.015	0.036	0.04	261	76	337	5	330	11	101.0

Plesovice160	9	759	0.0535	0.0009	0.394	0.014	0.055	0.04	320	73	337	5	336	11	99.1
Plesovice161	9	752	0.0539	0.0008	0.402	0.015	0.047	0.04	329	76	338	5	340	11	98.5
Plesovice162	9	754	0.0535	0.0009	0.401	0.016	0.160	0.04	350	78	336	5	342	12	97.1
Plesovice163	9	756	0.0539	0.0008	0.395	0.015	0.006	0.04	301	76	338	5	337	11	99.4
Plesovice164	9	760	0.0537	0.0008	0.393	0.014	0.097	0.04	307	73	337	5	335	10	99.5
Plesovice165	9	750	0.0534	0.0009	0.387	0.015	0.135	0.04	274	77	335	5	330	11	100.5
Plesovice166	9	751	0.0537	0.0008	0.396	0.015	0.038	0.04	314	76	337	5	337	11	99.0
Plesovice167	9	763	0.0538	0.0008	0.394	0.015	0.111	0.04	297	75	338	5	336	11	99.8
Plesovice168	9	753	0.0536	0.0009	0.399	0.014	0.049	0.04	340	79	337	6	340	10	98.0
Plesovice169	11	787	0.0537	0.0009	0.397	0.015	0.080	0.04	309	81	337	6	339	11	98.4
Plesovice170	11	750	0.0537	0.0009	0.399	0.015	0.142	0.04	314	81	337	5	340	11	98.1
Plesovice171	11	740	0.0536	0.0009	0.384	0.015	0.020	0.04	258	78	337	5	328	11	101.6
Plesovice172	11	768	0.0537	0.0009	0.401	0.015	0.129	0.04	332	80	337	5	342	11	97.7
Plesovice173	11	754	0.0537	0.0009	0.381	0.016	0.123	0.04	252	87	337	6	327	12	101.9
Plesovice174	11	745	0.0537	0.0009	0.394	0.016	0.044	0.04	330	85	337	6	336	11	99.3
Plesovice175	11	762	0.0537	0.0009	0.382	0.017	0.074	0.04	244	89	337	5	325	12	102.6
Plesovice176	11	750	0.0537	0.0009	0.394	0.016	0.140	0.04	300	80	337	6	335	11	99.6
Plesovice177	11	743	0.0537	0.0009	0.401	0.016	0.103	0.04	325	84	337	5	341	12	97.9
Plesovice178	11	758	0.0536	0.0010	0.394	0.016	0.105	0.04	329	86	336	6	337	12	98.8
Plesovice179	11	744	0.0537	0.0009	0.386	0.016	0.256	0.04	237	80	338	6	329	12	101.6
Plesovice180	11	740	0.0537	0.0009	0.398	0.017	0.218	0.04	344	83	337	6	340	12	98.1
Plesovice181	11	771	0.0537	0.0009	0.395	0.018	0.164	0.05	331	89	337	6	335	13	99.5
Plesovice182	11	758	0.0535	0.0009	0.394	0.017	0.118	0.04	301	86	336	6	334	12	99.6
Plesovice183	11	771	0.0541	0.0009	0.404	0.017	0.050	0.04	315	85	340	6	343	12	98.0
Plesovice184	11	740	0.0535	0.0009	0.390	0.016	0.170	0.04	273	83	336	6	331	12	100.4
Plesovice185	11	764	0.0536	0.0007	0.396	0.014	0.132	0.04	322	73	336	4	337	10	98.8
Plesovice186	11	767	0.0539	0.0006	0.394	0.015	0.220	0.04	287	73	339	4	334	11	100.3
Plesovice187	11	753	0.0537	0.0007	0.393	0.013	0.017	0.03	307	69	337	4	335	9	99.5
Plesovice188	11	755	0.0535	0.0007	0.393	0.015	0.032	0.04	302	81	336	4	336	11	98.9
Plesovice189	11	748	0.0537	0.0007	0.389	0.018	0.017	0.05	257	93	337	4	329	13	101.3
Plesovice190	11	763	0.0537	0.0007	0.400	0.014	0.252	0.04	338	69	337	4	340	10	98.2
Plesovice191	11	765	0.0537	0.0006	0.387	0.015	0.156	0.04	235	75	337	4	329	11	101.4
Plesovice192	11	754	0.0537	0.0007	0.397	0.013	0.125	0.03	304	70	337	4	338	10	98.9
Plesovice193	11	747	0.0537	0.0006	0.395	0.014	0.072	0.04	300	76	337	4	335	10	99.6
Plesovice194	11	759	0.0536	0.0007	0.392	0.014	0.042	0.04	281	77	336	4	335	10	99.4
Plesovice195	11	741	0.0539	0.0007	0.397	0.014	0.173	0.04	285	73	338	4	336	10	99.7
Plesovice196	11	751	0.0536	0.0007	0.389	0.014	0.011	0.04	295	77	336	4	333	10	100.0
Plesovice197	11	752	0.0536	0.0006	0.396	0.014	0.110	0.04	363	76	337	4	336	10	99.2
Plesovice198	11	756	0.0537	0.0006	0.394	0.014	0.153	0.04	357	74	337	4	336	10	99.3
Plesovice199	11	745	0.0536	0.0007	0.398	0.014	0.067	0.04	358	73	337	4	338	10	98.6
Plesovice200	11	749	0.0541	0.0007	0.392	0.013	0.001	0.03	264	72	339	4	333	10	100.8
Plesovice201	11	758	0.0532	0.0007	0.391	0.014	0.203	0.04	288	74	334	5	333	10	99.4
Plesovice202	11	804	0.0537	0.0007	0.392	0.016	0.005	0.04	266	80	337	4	333	11	100.2
Plesovice203	11	742	0.0539	0.0007	0.401	0.015	0.132	0.04	324	80	339	5	341	11	98.3
Plesovice204	11	730	0.0536	0.0006	0.395	0.013	0.141	0.03	307	70	337	4	336	10	99.2
Plesovice205	11	765	0.0535	0.0007	0.389	0.015	0.134	0.04	275	75	336	4	331	11	100.5
Plesovice206	11	771	0.0538	0.0006	0.395	0.013	0.106	0.03	317	71	338	4	336	10	99.5
Plesovice207	11	749	0.0534	0.0007	0.397	0.015	0.178	0.04	312	89	335	4	338	11	98.1

acorrected for background, instrumental drift and mass bias fractionation based on primary stantard.

c rho is the 207Pb/235U/206Pb/238U error correlation coefficient.

d degree of concordance: 100-((1+((206Pb/238U - 207Pb/235U)/206Pb/238U)) x 100)

Sample	Spot size (μm)	U (ppm)	$^{206}Pb^{a}/^{238}U$	±2s	$^{207}Pb^{a}/^{235}U$	±2s	Rho[c]	Th/U	$^{207}Pb/^{206}Pb$	±2s (Ma)	$^{206}Pb/^{238}U$	±2s (Ma)	$^{207}Pb/^{235}U$	±2s (Ma)	Conc.[d]
Secondaries															
BB9 1	11	388	0.0907	0.0020	0.731	0.031	0.138	0.04	490	76	559	12	553	18	100.1
BB9 2	11	400	0.0902	0.0020	0.700	0.030	0.128	0.04	397	78	557	12	532	18	103.4
BB9 3	11	406	0.0901	0.0020	0.739	0.029	0.162	0.04	529	73	556	12	559	18	98.5
BB9 4	11	410	0.0910	0.0021	0.758	0.032	0.185	0.04	544	78	562	12	566	18	98.2
BB9 5	11	403	0.0902	0.0020	0.735	0.030	0.241	0.04	508	76	557	12	556	18	99.1
BB9 6	11	414	0.0893	0.0020	0.695	0.028	0.275	0.04	415	70	551	12	534	16	102.1
BB9 7	11	454	0.0913	0.0014	0.718	0.036	0.284	0.05	409	97	563	8	543	21	102.6
BB9 8	11	466	0.0932	0.0014	0.731	0.034	0.228	0.05	416	91	574	8	552	20	102.9
BB9 9	11	431	0.0898	0.0012	0.721	0.035	0.110	0.05	451	95	554	7	546	21	100.4
BB9 10	11	444	0.0912	0.0013	0.725	0.036	0.186	0.05	419	95	563	8	547	21	101.8
BB9 11	11	439	0.0922	0.0013	0.748	0.037	0.212	0.05	457	96	569	8	560	21	100.5
BB9 12	11	431	0.0928	0.0015	0.783	0.040	0.256	0.05	550	100	572	9	579	23	97.7
BB9 13	11	431	0.0891	0.0016	0.718	0.025	0.275	0.03	496	77	550	9	544	15	100.1
BB9 14	11	434	0.0897	0.0016	0.753	0.027	0.167	0.04	569	75	554	10	565	16	97.0
BB9 15	11	448	0.0910	0.0016	0.724	0.025	0.182	0.03	464	74	561	9	548	15	101.3
BB9 16	9	421	0.0908	0.0014	0.715	0.038	0.165	0.05	449	130	560	9	544	23	101.9
BB9 17	9	425	0.0905	0.0014	0.741	0.039	0.166	0.05	527	140	558	8	559	23	98.9
BB9 18	9	417	0.0913	0.0015	0.747	0.040	0.223	0.05	486	130	563	9	561	23	99.3
BB9 19	9	418	0.0900	0.0015	0.731	0.038	0.198	0.05	465	130	555	9	552	22	99.6
BB9 20	9	418	0.0906	0.0015	0.728	0.039	0.140	0.05	471	130	559	9	555	24	99.7
BB9 21	9	425	0.0903	0.0015	0.732	0.040	0.265	0.05	480	130	557	9	554	23	99.5
BB9 22	9	406	0.0901	0.0010	0.737	0.029	0.230	0.04	516	84	556	6	556	18	99.0
BB9 23	9	411	0.0912	0.0011	0.758	0.031	0.234	0.04	547	83	563	6	570	18	97.7
BB9 24	9	445	0.0919	0.0011	0.757	0.029	0.270	0.04	531	77	567	7	567	17	98.9
BB9 25	11	404	0.0903	0.0019	0.723	0.027	0.259	0.04	476	76	557	11	550	16	100.3

BB9 26	11	410	0.0908	0.0019	0.763	0.031	0.304	0.04	553	83	560	11	570	18	97.2
BB9 27	11	404	0.0910	0.0020	0.709	0.027	0.129	0.04	436	74	562	12	539	16	103.0
BB9 28	11	420	0.0901	0.0020	0.732	0.028	0.313	0.04	520	78	556	12	553	16	99.5
BB9 29	11	398	0.0909	0.0020	0.732	0.028	0.154	0.04	513	77	561	12	554	17	100.2
BB9 30	9	433	0.0896	0.0015	0.715	0.030	0.224	0.04	459	90	553	9	543	18	100.8
BB9 31	9	420	0.0902	0.0015	0.747	0.027	0.284	0.04	546	83	557	9	561	16	98.2
BB9 32	9	411	0.0899	0.0015	0.764	0.029	0.296	0.04	609	89	555	9	573	17	95.7
BB9 33	9	440	0.0892	0.0014	0.709	0.028	0.121	0.04	454	86	551	8	540	17	101.0
BB9 34	9	426	0.0898	0.0015	0.746	0.029	0.359	0.04	541	88	554	9	560	17	97.9
BB9 35	9	430	0.0914	0.0015	0.723	0.030	0.262	0.04	446	89	564	9	547	17	102.0
BB9 36	9	389	0.0905	0.0018	0.730	0.034	0.251	0.05	509	86	558	10	553	21	100.0
BB9 37	9	392	0.0900	0.0017	0.747	0.034	0.375	0.05	556	81	555	10	563	20	97.6
BB9 38	9	414	0.0921	0.0017	0.755	0.036	0.238	0.05	522	86	568	10	566	22	99.3
BB9 39	9	392	0.0892	0.0014	0.780	0.027	0.203	0.03	657	70	551	8	581	15	93.5
BB9 40	9	409	0.0893	0.0014	0.737	0.030	0.221	0.04	544	84	551	8	556	17	98.1
BB9 41	9	400	0.0909	0.0015	0.746	0.028	0.279	0.04	529	77	561	9	560	16	99.1
BB9 42	11	384	0.0914	0.0017	0.757	0.029	0.235	0.04	545	85	564	10	570	18	97.8
BB9 43	11	380	0.0918	0.0016	0.714	0.029	0.145	0.04	415	86	566	9	541	17	103.5
BB9 44	11	382	0.0922	0.0017	0.733	0.031	0.234	0.04	480	88	569	10	552	18	101.9
BB9 45	11	381	0.0909	0.0016	0.715	0.030	0.217	0.04	450	87	562	9	542	18	102.5
BB9 46	11	381	0.0917	0.0016	0.709	0.030	0.335	0.04	413	92	566	9	539	18	103.7
BB9 47	11	388	0.0913	0.0015	0.746	0.030	0.250	0.04	504	84	563	9	560	17	99.6
BB9 48	11	393	0.0892	0.0012	0.725	0.024	0.258	0.03	516	70	551	7	552	14	98.8
BB9 49	11	382	0.0928	0.0012	0.750	0.029	0.173	0.04	490	84	572	7	565	17	100.2
BB9 50	11	390	0.0908	0.0012	0.719	0.024	0.181	0.03	462	72	560	7	548	15	101.1
91500 1	11	75	0.1786	0.0047	1.790	0.110	0.170	0.06	860	120	1058	26	1013	41	103.3
91500 2	11	71	0.1758	0.0046	1.763	0.100	0.253	0.06	870	110	1043	25	1016	36	101.6
91500 3	11	71	0.1764	0.0049	1.890	0.110	0.278	0.06	990	120	1046	27	1049	39	98.7
91500 4	11	72	0.1830	0.0051	1.830	0.120	0.206	0.07	830	130	1082	28	1029	42	103.9
91500 5	11	71	0.1717	0.0048	1.722	0.100	0.199	0.06	860	120	1020	26	990	39	101.9
91500 6	11	74	0.1707	0.0046	1.756	0.100	0.206	0.06	910	120	1014	25	1016	39	98.8
91500 7	11	80	0.1749	0.0039	1.730	0.140	0.170	0.08	650	170	1037	21	957	56	106.7
91500 8	11	78	0.1773	0.0041	1.710	0.130	0.242	0.08	670	160	1050	23	959	52	107.7
91500 9	11	75	0.1741	0.0043	1.850	0.140	0.195	0.08	830	160	1032	24	1000	54	102.1
91500 10	11	82	0.1731	0.0041	1.670	0.130	0.166	0.08	630	170	1027	23	942	54	107.3
91500 11	11	76	0.1767	0.0045	1.860	0.150	0.184	0.08	820	160	1047	25	1006	55	102.9
91500 12	11	77	0.1785	0.0049	1.910	0.140	0.354	0.07	870	170	1056	27	1027	56	101.7
91500 13	11	81	0.1738	0.0041	1.900	0.110	0.280	0.06	970	130	1032	22	1044	41	97.8
91500 14	11	77	0.1772	0.0044	1.869	0.094	0.197	0.05	1000	100	1050	24	1051	33	98.9
91500 15	11	73	0.1782	0.0042	1.900	0.130	0.230	0.07	920	140	1056	23	1037	46	100.8
91500 16	9	92	0.1724	0.0035	1.806	0.120	0.216	0.07	950	160	1024	19	1028	44	98.6
91500 17	9	87	0.1763	0.0039	1.766	0.120	0.179	0.07	860	160	1045	21	1011	44	102.3
91500 18	9	86	0.1761	0.0037	1.736	0.110	0.278	0.06	820	150	1044	20	1001	39	103.1
91500 19	9	88	0.1770	0.0037	1.762	0.120	0.106	0.07	810	150	1049	20	1007	44	103.0
91500 20	9	88	0.1772	0.0040	1.737	0.110	0.217	0.06	820	150	1053	22	1002	43	103.8
91500 21	9	84	0.1758	0.0038	1.765	0.120	0.223	0.07	890	160	1043	21	1014	44	101.8
91500 22	9	73	0.1772	0.0035	1.817	0.100	0.242	0.06	910	120	1050	19	1032	36	100.7
91500 23	9	73	0.1773	0.0037	1.910	0.110	0.176	0.06	990	110	1050	20	1052	38	98.8
91500 24	9	74	0.1807	0.0035	1.774	0.100	0.164	0.06	820	120	1071	19	1011	39	104.6
91500 25	11	70	0.1795	0.0049	1.742	0.096	0.336	0.06	790	120	1063	27	997	36	105.2
91500 26	11	78	0.1729	0.0047	1.816	0.100	0.160	0.06	960	120	1027	26	1027	39	99.0
91500 27	11	72	0.1774	0.0049	1.770	0.110	0.206	0.06	860	120	1051	27	1009	39	103.0
91500 28	11	81	0.1721	0.0046	1.830	0.110	0.264	0.06	990	120	1022	25	1036	38	97.6
91500 29	11	69	0.1808	0.0048	1.725	0.098	0.221	0.06	800	120	1070	26	995	39	106.0
91500 30	9	72	0.1736	0.0040	1.760	0.110	0.144	0.06	880	140	1033	22	1004	45	101.8
91500 31	9	82	0.1753	0.0040	1.767	0.098	0.313	0.06	880	120	1040	22	1012	37	101.7
91500 32	9	77	0.1740	0.0038	1.810	0.100	0.320	0.06	950	120	1033	21	1027	36	99.6
91500 33	9	76	0.1783	0.0042	1.920	0.130	0.205	0.07	990	150	1057	23	1058	47	98.9
91500 34	9	73	0.1761	0.0041	1.780	0.110	0.271	0.06	840	130	1044	23	1004	40	102.8
91500 35	9	73	0.1749	0.0041	1.800	0.110	0.306	0.06	890	140	1038	22	1008	42	101.9
91500 36	9	77	0.1737	0.0041	1.861	0.110	0.289	0.06	1010	110	1031	23	1043	39	97.8
91500 37	9	78	0.1794	0.0044	2.530	0.200	-0.085	0.08	1430	130	1062	24	1231	56	83.1
91500 38	9	77	0.1700	0.0041	1.800	0.110	0.160	0.06	1000	110	1011	23	1027	40	97.4
91500 39	9	77	0.1746	0.0036	1.874	0.100	0.286	0.05	1000	110	1038	20	1048	36	98.0
91500 40	9	77	0.1747	0.0037	1.733	0.093	0.281	0.05	820	110	1036	20	992	34	103.2
91500 41	9	77	0.1757	0.0039	1.773	0.093	0.234	0.05	900	110	1042	21	1019	34	101.2
91500 42	11	67	0.1760	0.0044	1.749	0.100	0.318	0.06	850	120	1043	24	1000	39	103.1
91500 43	11	65	0.1746	0.0043	1.746	0.100	0.231	0.06	840	120	1036	24	991	40	103.3
91500 44	11	63	0.1745	0.0041	1.681	0.095	0.273	0.06	820	120	1035	22	979	37	104.4
91500 45	11	68	0.1738	0.0042	1.820	0.110	0.159	0.06	960	120	1031	23	1026	40	99.5
91500 46	11	65	0.1728	0.0042	1.870	0.110	0.288	0.06	970	130	1026	23	1040	40	97.6
91500 47	11	70	0.1727	0.0042	1.730	0.110	0.228	0.06	830	130	1025	23	983	42	103.1
91500 48	11	69	0.1789	0.0036	1.800	0.100	0.098	0.06	850	120	1059	20	1012	39	103.4
91500 49	11	69	0.1787	0.0036	1.930	0.100	0.279	0.05	980	120	1059	20	1059	37	99.0
91500 50	11	77	0.1809	0.0037	1.899	0.097	0.167	0.05	970	110	1070	20	1060	35	99.9
GJ1 1	11	343	0.0968	0.0023	0.973	0.040	0.370	0.04	937	80	595	13	684	21	84.1
GJ1 2	11	347	0.0931	0.0021	0.776	0.032	0.216	0.04	564	73	573	13	577	18	98.4
GJ1 3	11	344	0.0936	0.0022	0.758	0.032	0.212	0.04	484	77	577	13	566	19	100.9
GJ1 4	11	343	0.0942	0.0021	0.799	0.032	0.268	0.04	586	74	580	12	590	18	97.3
GJ1 5	11	341	0.0936	0.0021	0.729	0.031	0.135	0.04	406	77	576	13	549	19	103.8

GJ1 6	11	345	0.0938	0.0021	0.798	0.033	0.207	0.04	605	77	578	12	592	19	96.6
GJ1 7	11	361	0.0963	0.0017	0.834	0.041	0.257	0.05	NAN	99	592	10	609	23	96.1
GJ1 8	11	353	0.0969	0.0014	0.799	0.040	0.311	0.05	NAN	100	596	8	588	23	100.4
GJ1 9	11	353	0.0968	0.0016	0.764	0.040	0.204	0.05	NAN	100	596	9	565	23	104.1
GJ1 10	11	354	0.0983	0.0016	0.803	0.041	0.195	0.05	NAN	99	604	10	587	23	101.8
GJ1 11	11	363	0.0966	0.0016	0.825	0.041	0.243	0.05	NAN	100	594	9	602	23	97.7
GJ1 12	11	353	0.0975	0.0015	0.798	0.045	0.221	0.06	NAN	110	599	9	582	25	101.9
GJ1 13	9	341	0.0943	0.0015	0.761	0.041	0.099	0.05	NAN	76	581	9	572	24	100.5
GJ1 14	9	337	0.0944	0.0016	0.782	0.042	0.267	0.05	NAN	77	581	9	582	24	98.9
GJ1 15	9	344	0.0927	0.0015	0.768	0.042	0.283	0.05	NAN	78	572	9	574	24	98.6
GJ1 16	9	339	0.0949	0.0017	0.768	0.041	0.329	0.05	NAN	78	584	10	576	24	100.4
GJ1 17	9	350	0.0936	0.0016	0.799	0.045	0.106	0.06	NAN	80	577	9	590	25	96.7
GJ1 18	9	343	0.0931	0.0015	0.769	0.044	0.214	0.06	NAN	89	574	9	573	26	99.1
GJ1 19	9	328	0.0983	0.0016	0.791	0.028	0.379	0.04	499	84	604	10	589	16	101.5
GJ1 20	9	328	0.0975	0.0017	0.794	0.033	0.102	0.04	494	87	600	10	587	18	101.1
GJ1 21	9	326	0.0981	0.0017	0.833	0.034	0.204	0.04	585	88	603	10	610	19	97.8
GJ1 22	9	323	0.0965	0.0017	0.793	0.034	0.243	0.04	521	94	594	10	589	19	99.8
GJ1 23	9	332	0.0971	0.0017	0.796	0.035	0.151	0.04	504	93	597	10	588	20	100.5
GJ1 24	9	338	0.0973	0.0016	0.810	0.032	0.291	0.04	554	87	598	10	596	18	99.4
GJ1 25	11	318	0.0972	0.0018	0.816	0.034	0.278	0.04	563	89	598	11	598	19	98.9
GJ1 26	11	321	0.0960	0.0017	0.782	0.032	0.205	0.04	503	88	591	10	580	18	100.9
GJ1 27	11	331	0.0964	0.0017	0.788	0.032	0.201	0.04	503	86	593	10	584	18	100.5
GJ1 28	11	321	0.0969	0.0017	0.801	0.032	0.188	0.04	524	84	596	10	592	18	99.7
GJ1 29	11	321	0.0983	0.0017	0.823	0.032	0.219	0.04	589	84	604	10	605	18	98.9
GJ1 30	11	322	0.0990	0.0017	0.794	0.033	0.075	0.04	509	86	608	10	586	19	102.7
Temora 1	11	203	0.0668	0.0018	0.481	0.034	0.307	0.07	210	130	417	11	386	23	106.3
Temora 2	11	267	0.0672	0.0017	0.476	0.027	0.262	0.06	210	100	419	10	391	18	105.7
Temora 3	11	195	0.0654	0.0018	0.508	0.039	0.245	0.08	320	140	408	11	404	26	100.0
Temora 4	11	209	0.0669	0.0017	0.526	0.036	0.114	0.07	380	130	417	10	417	24	99.0
Temora 5	11	164	0.0676	0.0019	0.529	0.040	0.121	0.08	340	140	421	11	415	27	100.5
Temora 6	11	128	0.0653	0.0018	0.509	0.043	0.230	0.08	340	160	407	11	403	30	100.0
Temora 7	11	213	0.0654	0.0015	0.537	0.051	0.255	0.09	280	190	408	9	411	34	98.3
Temora 8	11	242	0.0673	0.0014	0.506	0.043	0.170	0.08	180	160	420	8	395	29	104.9
Temora 9	11	136	0.0674	0.0016	0.546	0.070	0.123	0.13	130	250	420	10	399	50	104.0
Temora 10	11	221	0.0667	0.0014	0.513	0.044	0.233	0.09	220	170	416	9	405	30	101.6
Temora 11	11	139	0.0678	0.0018	0.474	0.061	0.290	0.13	-100	240	422	11	346	46	117.0
Temora 12	11	125	0.0661	0.0018	0.555	0.071	0.323	0.13	160	250	413	11	406	48	100.7
Temora 13	11	207	0.0643	0.0015	0.494	0.034	0.312	0.07	330	140	402	9	400	23	99.4
Temora 14	11	200	0.0659	0.0014	0.486	0.038	0.110	0.08	230	140	411	9	389	26	104.4
Temora 15	11	178	0.0646	0.0015	0.503	0.040	0.211	0.08	330	150	403	9	395	28	101.1
Temora 16	9	271	0.0640	0.0012	0.515	0.034	0.219	0.07	420	150	400	7	418	23	94.4
Temora 17	9	402	0.0639	0.0012	0.493	0.029	0.266	0.06	377	140	399	7	403	20	98.0
Temora 18	9	174	0.0678	0.0016	0.473	0.037	0.128	0.08	160	140	423	10	386	25	107.7
Temora 19	9	144	0.0628	0.0030	0.509	0.076	0.401	0.15	450	320	392	18	409	56	94.7
Temora 20	9	140	0.0671	0.0017	0.474	0.044	0.239	0.09	160	160	419	10	380	30	108.2
Temora 21	9	179	0.0664	0.0016	0.515	0.037	0.192	0.07	340	140	414	10	410	25	100.0
Temora 22	9	105	0.0656	0.0018	0.475	0.053	0.291	0.11	160	190	409	11	370	39	108.6
Temora 23	9	137	0.0672	0.0016	0.484	0.045	0.187	0.09	170	170	419	10	383	32	107.6
Temora 24	11	225	0.0663	0.0014	0.530	0.033	0.312	0.06	440	120	414	9	423	22	96.8
Temora 25	11	156	0.0671	0.0015	0.494	0.039	0.245	0.08	250	140	418	9	394	27	104.8
Temora 26	11	178	0.0672	0.0016	0.483	0.036	0.328	0.07	190	140	419	10	385	24	107.1
Temora 27	11	211	0.0659	0.0014	0.479	0.030	0.198	0.06	260	120	411	8	393	20	103.4
Temora 28	11	285	0.0667	0.0013	0.521	0.027	0.293	0.05	428	100	416	8	419	18	98.3
Temora 29	11	189	0.0671	0.0015	0.492	0.033	0.193	0.07	280	130	419	9	400	23	103.4

acorrected for background, instrumental drift and mass bias fractionation based on primary stantard.

c rho is the 207Pb/235U/206Pb/238U error correlation coefficient.

d degree of concordance: 100-((1+((206Pb/238U - 207Pb/235U)/206Pb/238U)) x 100)

Rutile

Sample	Spot size (µm)	U (ppm)	$^{206}Pb^{a}/^{238}U$	±2s	$^{207}Pb^{a}/^{235}U$	±2s	Rho[c]	^{206}Pb common	$^{207}Pb/^{206}Pb$	±2s (Ma)	$^{206}Pb/^{238}U$	±2s (Ma)	$^{207}Pb/^{235}U$	±2s (Ma)	Conc.[d]
AB-07-09															
U10a	20	83.1	14.472	0.545	0.057	0.002	0.122	1.2	448	60	431	16	437	20	97.5
U13a	20	91.5	11.655	0.462	0.184	0.009	-0.712	19.1	2604	80	530	20	1157	54	-19.2
U13b	20	98.7	14.339	0.535	0.055	0.002	0.254	0.0	377	66	435	16	430	20	100.0
U3a	20	125.5	14.318	0.533	0.060	0.001	-0.017	1.0	572	53	435	16	463	21	92.6
U5a	20	103.9	13.974	0.527	0.056	0.002	0.124	1.6	430	61	446	16	447	21	98.8
U6a	20	129.7	14.325	0.534	0.057	0.001	0.338	0.0	464	53	435	16	444	20	97.0
U7a	20	150.4	9.050	0.352	0.342	0.008	-0.185	34.9	3666	32	676	25	1847	44	-74.4
U8a	20	145.8	14.616	0.555	0.055	0.002	0.082	1.9	375	63	427	16	423	19	99.8
U02a	20	140.3	14.562	0.657	0.055	0.001	0.154	0.0	404	57	428	19	428	25	99.0
U04a	20	169.8	13.966	0.644	0.061	0.002	0.038	0.0	604	75	446	20	482	29	90.9
U06b	20	129	14.280	0.653	0.054	0.002	0.160	1.7	360	58	436	19	429	25	100.7
U08c	20	139.9	12.853	0.595	0.113	0.005	-0.331	7.9	1792	79	483	22	801	47	33.2
U10b	20	84.2	14.239	0.649	0.055	0.002	0.301	1.0	381	71	438	19	435	26	99.5
U10c	20	76.2	13.405	0.629	0.081	0.003	0.144	2.4	1162	84	464	21	606	37	68.4
U11a	20	160.3	15.060	0.726	0.056	0.004	0.357	0.1	400	140	415	19	429	32	95.6
U12a	20	189.5	14.663	0.688	0.057	0.002	0.186	0.0	481	70	425	19	443	27	94.9

Primary															
R10_1	20	0.001	5.429	0.088	0.076	0.001	0.115	44.66	1073	28	1089	17	1087	37	99.2
R10_2	20	0.000	5.426	0.088	0.076	0.001	0.201	43.91	1085	29	1090	17	1089	37	99.1
R10_3	20	0.000	5.385	0.090	0.076	0.001	0.352	43.02	1079	28	1098	17	1090	36	99.7
R10_4	20	0.000	5.411	0.091	0.076	0.001	0.176	44.91	1079	31	1093	18	1089	38	99.4
R10_5	20	0.001	5.444	0.089	0.076	0.001	0.306	44.35	1082	30	1087	17	1084	36	99.3
R10_6	20	0.000	5.368	0.089	0.076	0.001	0.168	44.03	1080	27	1101	17	1093	36	99.7
R10_7	20	0.000	5.470	0.090	0.076	0.001	0.169	44.15	1073	28	1082	17	1089	36	98.4
R10_8	20	0.000	5.476	0.090	0.076	0.001	0.032	43.81	1081	29	1081	17	1087	39	98.4
R10_9	20	0.000	5.359	0.089	0.076	0.001	0.156	44.6	1077	31	1102	17	1091	40	100.0
R10_10	20	0.000	5.417	0.091	0.076	0.001	0.075	43.9	1076	32	1092	18	1087	40	99.5
R10_11	20	0.000	5.417	0.091	0.076	0.001	0.073	43.77	1075	32	1092	18	1087	39	99.5
R10_12	20	0.000	5.461	0.092	0.076	0.001	0.229	44.56	1071	30	1085	18	1087	37	98.8
R10_13	20	0.000	5.400	0.087	0.076	0.001	0.143	44.08	1071	37	1095	17	1088	43	99.6
R10_14	20	0.000	5.400	0.087	0.076	0.001	0.144	43.95	1068	36	1095	17	1087	42	99.7
R10_15	20	0.001	5.311	0.203	0.076	0.002	0.125	44.53	1090	42	1111	39	1108	36	99.3
R10_16	20	0.001	5.308	0.203	0.076	0.002	0.123	44.38	1088	42	1112	39	1107	36	99.4
R10_17	20	0.000	5.510	0.212	0.076	0.002	0.291	43.94	1073	46	1075	38	1076	37	98.9
R10_18	20	0.000	5.513	0.213	0.076	0.002	0.291	43.86	1073	46	1074	38	1075	37	98.9
R10_19	20	0.000	5.510	0.212	0.076	0.002	0.152	41.86	1074	43	1074	38	1073	37	99.1
R10_20	20	0.000	5.504	0.212	0.076	0.002	0.049	46.04	1063	52	1076	38	1079	38	98.7
R10_21	20	0.000	5.373	0.202	0.076	0.002	0.342	44.57	1086	45	1100	38	1102	35	98.8
R10_22	20	0.000	5.453	0.205	0.076	0.002	0.108	43.06	1065	45	1085	37	1079	36	99.6
R10_23	20	0.000	5.328	0.202	0.077	0.002	0.311	45.09	1095	43	1109	39	1111	36	98.8
R10_24	20	0.000	5.400	0.210	0.073	0.002	0.223	42.87	1013	52	1095	39	1070	37	101.3
R10_25	20	0.000	5.441	0.204	0.075	0.002	0.075	45.78	1059	44	1087	38	1082	36	99.5
R10_26	20	0.000	5.371	0.202	0.076	0.002	0.158	43.76	1086	42	1100	38	1096	37	99.4
R10_27	20	0.000	5.429	0.209	0.077	0.002	0.007	43.43	1097	47	1089	38	1095	37	98.4
R10_28	20	0.000	5.565	0.207	0.076	0.002	0.417	43.53	1068	46	1065	37	1071	36	98.5
R10_29	20	0.002	5.305	0.200	0.076	0.002	0.385	44.95	1084	47	1113	38	1106	37	99.6
R10_30	20	0.000	5.227	0.251	0.075	0.003	0.143	43.2	1050	70	1130	48	1098	50	101.8
R10_31	20	0.000	5.568	0.254	0.074	0.002	0.205	43.1	1023	54	1064	45	1051	49	100.2
R10_32	20	0.002	5.294	0.241	0.077	0.002	0.244	46.6	1094	48	1115	47	1113	47	99.2
R10_33	20	0.000	5.408	0.249	0.077	0.002	0.168	44.9	1081	52	1093	46	1093	48	99.0
R10_34	20	0.000	5.473	0.249	0.076	0.002	0.005	44.1	1076	51	1081	46	1086	48	98.5
R10_35	20	0.000	5.543	0.258	0.076	0.002	0.158	43.87	1065	54	1069	46	1075	50	98.4
R10_36	20	0.000	5.236	0.241	0.077	0.002	0.137	43.9	1099	51	1126	48	1127	49	98.9
R10_37	20	0.000	5.513	0.252	0.076	0.002	0.255	43.7	1071	54	1074	45	1076	48	98.8
R10_38	20	0.000	5.277	0.242	0.075	0.002	0.157	43.3	1053	56	1118	47	1101	48	100.5
R10_39	20	0.000	5.459	0.247	0.076	0.002	0.163	44.9	1065	48	1084	46	1081	47	99.3
R10_40	20	0.000	5.459	0.247	0.075	0.002	0.232	42.4	1039	53	1084	45	1070	48	100.3
R10_41	20	0.000	5.423	0.247	0.075	0.002	0.273	45.3	1049	53	1091	46	1079	48	100.1
R10_42	20	0.000	5.464	0.251	0.076	0.002	0.171	44.3	1072	53	1083	46	1085	48	98.8
R10_43	20	0.000	5.382	0.246	0.077	0.002	0.092	44.3	1099	49	1098	47	1105	47	98.4
Secondaries															
SAE1	20	0.000	11.862	0.197	0.057	0.002	0.151	41.59	464	57	521.7	8.2	514	19	100.5
SAE2	20	0.000	11.920	0.199	0.057	0.001	0.146	43.4	444	54	519.2	8.2	508	18	101.2
SAE3	20	0.000	11.662	0.190	0.056	0.001	0.200	39.16	426	57	530.3	8.5	514	18	102.1
SAE4	20	0.000	11.825	0.196	0.057	0.002	0.249	42.05	434	56	523.3	8.2	508.2	18	101.9
SAE5	20	0.000	12.011	0.202	0.057	0.002	-0.009	42.76	457	55	515.5	8.3	512	20	99.7
SAE6	20	0.000	11.236	0.202	0.057	0.002	0.046	23.84	444	69	549.7	9.4	543	25	100.2
SAE7	20	0.000	10.929	0.203	0.056	0.002	0.242	19.47	396	81	564.4	9.9	543	27	102.8
SAE8	20	0.000	10.953	0.192	0.058	0.002	0.208	22.1	456	77	562.8	9.7	545	27	102.2
SAE9	20	0.000	11.211	0.214	0.056	0.002	0.313	23.52	404	78	550.4	10	522	24	104.2
SAE10	20	0.000	11.038	0.207	0.057	0.002	0.293	23.46	434	71	559	9.9	536	22	103.1
SAE11	20	0.000	10.965	0.192	0.057	0.002	0.083	19.62	414	81	562.3	9.7	545	28	102.1
SAE12	20	0.000	11.086	0.209	0.058	0.002	0.249	20.16	467	76	556.4	10	550	26	100.2
SAE13	20	0.000	12.028	0.448	0.058	0.002	0.162	43.79	466	71	514.8	19	510	24	99.9
SAE14	20	0.000	12.180	0.460	0.058	0.002	0.311	43.67	480	76	508.5	19	509	24	98.9
SAE15	20	0.000	12.372	0.474	0.056	0.002	0.149	40.16	415	75	501.7	18	496	23	100.1
SAE16	20	0.000	12.086	0.453	0.056	0.002	0.206	39.97	406	76	512.4	19	500	24	101.4
SAE17	20	0.000	11.947	0.457	0.058	0.002	0.131	38.63	477	71	518.1	19	517	24	99.2
SAE18	20	0.000	12.303	0.469	0.056	0.002	0.142	38.9	399	77	503.7	19	492	24	101.3
SAE19	20	0.000	12.015	0.462	0.056	0.002	0.310	39.06	391	77	515.3	19	500	24	102.0
SAE20	20	0.000	12.435	0.464	0.057	0.002	0.206	48.66	444	67	498.5	18	495	23	99.7
SAE21	20	0.000	11.990	0.460	0.058	0.002	0.141	48.19	484	67	516.1	19	516	24	99.0
SAE22	20	0.000	12.013	0.462	0.057	0.002	0.143	43.65	446	70	515.3	19	508	23	100.4
SAE23	20	0.000	11.891	0.452	0.056	0.002	0.221	38.29	387	74	520.2	19	502	24	102.5
SAE24	20	0.000	12.438	0.572	0.058	0.002	0.290	37.61	465	83	498.5	22	501	30	98.5
SAE25	20	0.000	12.466	0.575	0.059	0.002	-0.012	43.22	513	76	497.3	22	508	30	96.8
SAE26	20	0.000	12.107	0.557	0.056	0.002	0.275	38.01	412	89	511.3	23	500	32	101.2
SAE27	20	0.000	12.429	0.572	0.059	0.002	0.219	37.08	479	87	498.8	22	505	31	97.8
SAE28	20	0.000	12.019	0.549	0.058	0.003	0.162	35.39	453	93	514.9	23	511	33	99.8
SAE29	20	0.000	12.048	0.552	0.057	0.002	0.138	41.86	428	89	513.9	23	500	31	101.7
SAE30	20	0.000	12.210	0.567	0.056	0.002	0.200	42.94	404	86	507.1	23	494	30	101.6
SAE31	20	0.000	12.330	0.578	0.058	0.002	0.261	40.43	462	89	502.6	23	504	31	98.7
SAE32	20	0.000	12.210	0.567	0.060	0.002	0.179	43.11	543	85	507.4	22	522	32	96.1
SAE33	20	0.000	12.183	0.549	0.058	0.003	0.133	41.83	429	97	508.4	22	503	32	100.1
SAE34	20	0.003	12.005	0.548	0.058	0.002	0.158	42.75	483	85	515.9	23	517	32	98.8
R632_1	20	0.005	10.891	0.166	0.064	0.002	0.156	215	722	49	566	8	600	21	93.0

R632_2	20	0.024	11.246	0.190	0.063	0.001	0.142	224	678	44	549	9	583	19	92.9
R632_3	20	0.000	11.157	0.174	0.058	0.001	0.324	226	500	28	553	8	552	13	99.2
R632_4	20	0.001	11.371	0.181	0.057	0.001	0.249	223	465	27	543	8	530	11	101.5
R632_5	20	0.000	12.247	0.180	0.056	0.001	0.111	411	465	19	506	7	495	9	101.2
R632_6	20	0.000	12.157	0.177	0.057	0.001	0.227	430	471	20	510	7	501	10	100.7
R632_7	20	0.000	11.833	0.182	0.057	0.000	0.407	427	480	19	523	8	517	9	100.1
R632_8	20	0.000	12.074	0.175	0.058	0.001	0.281	430	511	20	513	7	520	10	97.7
R632_9	20	0.023	12.174	0.193	0.058	0.001	0.561	429	514	22	509	8	514	10	98.0
R632_10	20	0.031	12.034	0.463	0.057	0.001	-0.005	512	475	46	515	19	510	22	99.9
R632_11	20	0.000	12.045	0.450	0.057	0.001	0.257	467	494	40	514	18	513	20	99.1
R632_12	20	0.001	12.149	0.458	0.057	0.001	0.338	473	503	38	510	18	511	21	98.8
R632_13	20	0.005	12.338	0.548	0.057	0.001	0.098	431	490	42	502	22	503	27	98.9
R632_14	20	0.021	12.206	0.551	0.057	0.001	0.129	420	463	44	508	22	500	28	100.5
R632_15	20	0.001	12.114	0.543	0.058	0.001	-0.011	454	505	44	511	22	516	29	98.0
R13_1	20	0.000	12.438	0.248	0.059	0.002	0.238	15.68	477	83	498.1	9.4	507	26	97.2
R13_2	20	0.055	12.048	0.232	0.062	0.003	0.156	15.99	608	85	513.7	9.4	536	30	94.7
R13_3	20	0.000	11.962	0.243	0.056	0.002	0.152	16.52	411	90	518.1	10	507	28	101.1
R13_4	20	0.000	11.919	0.227	0.055	0.002	0.257	16.28	339	83	519.3	9.4	495	26	103.7
R13_5	20	0.000	14.535	0.592	0.055	0.003	0.153	15.67	320	120	428.6	17	386	25	108.9
R13_6	20	0.000	14.577	0.616	0.059	0.003	0.107	17.92	450	100	427.6	17	406	24	104.1
R13_7	20	0.000	12.579	0.601	0.056	0.003	0.142	16.24	380	120	493.8	23	481	33	101.6
R13_8	20	0.000	12.165	0.592	0.055	0.003	0.288	16.43	340	120	510.1	23	488	33	103.3
R19_1	20	0.014	12.330	0.258	0.059	0.003	0.225	15.6	469	96	502.3	10	506	30	98.3
R19_2	20	0.003	12.484	0.265	0.058	0.002	0.253	16.4	427	90	496.5	10	491	28	100.1
R19_3	20	0.001	12.674	0.241	0.055	0.002	0.239	16.0	375	88	489.2	9.1	475	26	101.9
R19_4	20	0.001	12.407	0.246	0.058	0.003	0.106	14.9	429	92	499.2	9.7	500	29	98.8
R19_5	20	0.000	15.576	0.655	0.057	0.003	0.210	14.3	360	110	400.6	16	365	23	107.9
R19_6	20	0.001	15.723	0.643	0.058	0.003	0.164	15.7	410	110	397.2	16	378	24	103.8
R19_7	20	0.003	15.870	0.630	0.059	0.003	0.118	17.1	460	110	393.8	16	391	25	99.7
R19_8	20	0.002	13.369	0.661	0.057	0.003	0.278	15.7	390	120	464.8	22	460	34	100.0
R19_9	20	0.017	12.092	0.570	0.056	0.004	0.252	15.7	320	140	512	23	488	37	103.7
R19_10	20	0.009	12.739	0.617	0.059	0.004	0.189	16.3	420	120	486.9	23	490	36	98.4

[a]corrected for background, instrumental drift and mass bias fractionation based on primary stantard.

[c] rho is the 207Pb/235U/206Pb/238U error correlation coefficient.

[d] degree of concordance: 100-((1+((206Pb/238U - 207Pb/235U)/206Pb/238U)) x 100)

Monazite															
Sample	U (ppm)	$^{207}Pb^a/^{206}Pb$	±2s	$^{208}Pb^a/^{232}Th$	±2s	$^{207}Pb^a/^{235}U$	±2s	$^{206}Pb^a/^{238}U$	±2s	Rho[c]	$^{206}Pb/^{238}U$	±2s (Ma)	$^{207}Pb/^{235}U$	±2s (Ma)	Conc.[d]
Sample															
RunD															
RS-14-16_M02	1118	0.0562	0.0028	0.02765	0.00065	0.527	0.025	0.0674	0.0018	0.1450	420	11	424	17	99.1
RS-14-16_M03	697	0.0543	0.0034	0.02775	0.00056	0.523	0.034	0.0681	0.0020	0.2805	425	12	419	23	101.3
RS-14-16_M04	893	0.0573	0.0034	0.02725	0.00056	0.532	0.031	0.0661	0.0019	0.1290	413	11	424	21	97.2
RS-14-16_M05	1344	0.0570	0.0022	0.02771	0.00053	0.533	0.022	0.0674	0.0018	0.2849	421	11	431	15	97.5
RS-14-16_M06	1014	0.0609	0.0044	0.02929	0.00079	0.554	0.036	0.0668	0.0020	0.0874	417	12	441	23	94.2
RS-14-16_M07	816	0.0541	0.0034	0.02689	0.00054	0.493	0.031	0.0663	0.0019	0.1764	413	11	401	22	103.0
RS-14-16_M08	428	0.0542	0.0049	0.02676	0.00057	0.518	0.047	0.0676	0.0021	0.2010	421	13	402	31	104.5
RS-14-16_M09	1001	0.0581	0.0030	0.02722	0.00056	0.552	0.029	0.0680	0.0018	0.1901	424	11	438	19	96.6
RS-14-16_M12	247	0.0546	0.0060	0.02711	0.00049	0.570	0.062	0.0756	0.0028	0.1486	469	17	444	40	105.3
RS-14-16_M13	78	0.0650	0.0170	0.02777	0.00062	0.550	0.140	0.0685	0.0039	0.0814	428	24	400	93	106.5
RS-14-16_M15	250	0.0551	0.0067	0.02701	0.00062	0.516	0.059	0.0694	0.0026	0.0154	432	15	400	41	107.4
RS-14-16_M16	416	0.0563	0.0048	0.02733	0.00053	0.532	0.045	0.0680	0.0021	0.1197	424	13	414	30	102.4
RunC															
RS-14-16_M02	1098	0.0579	0.0026	0.02770	0.00052	0.527	0.052	0.0667	0.0061	0.2114	416	37	427	35	97.4
RS-14-16_M03	687	0.0586	0.0031	0.02729	0.00058	0.535	0.055	0.0667	0.0061	0.0791	416	37	431	35	96.4
RS-14-16_M04	859	0.0572	0.0027	0.02846	0.00061	0.519	0.052	0.0665	0.0061	0.1641	415	37	419	34	99.0
RS-14-16_M05	1002	0.0573	0.0027	0.02721	0.00050	0.512	0.050	0.0657	0.0060	0.1472	410	36	418	35	98.1
RS-14-16_M06	853	0.0566	0.0029	0.02757	0.00068	0.501	0.051	0.0652	0.0060	0.3231	407	36	409	35	99.4
RS-14-16_M07	803	0.0563	0.0029	0.02704	0.00054	0.506	0.052	0.0657	0.0060	0.1111	410	36	412	36	99.5
RS-14-16_M08	848	0.0594	0.0046	0.02908	0.00078	0.516	0.060	0.0643	0.0060	0.1472	401	36	420	41	95.3
RS-14-16_M09	894	0.0547	0.0027	0.02629	0.00052	0.492	0.050	0.0653	0.0060	0.2802	408	36	401	34	101.6
RS-14-16_M12	477	0.0581	0.0041	0.02815	0.00057	0.544	0.061	0.0688	0.0064	0.1986	429	38	432	41	99.3
RS-14-16_M13	72	0.0610	0.0180	0.02698	0.00057	0.560	0.150	0.0694	0.0072	0.1104	431	43	270	120	137.4
RS-14-16_M15	233	0.0656	0.0075	0.02772	0.00055	0.585	0.082	0.0670	0.0064	0.0050	418	38	443	54	94.0
RS-14-16_M16	428	0.0581	0.0044	0.02751	0.00055	0.520	0.059	0.0671	0.0062	0.1088	418	38	423	42	98.8
RunB															
RS-14-16_M13c	79	0.0562	0.0012			0.507	0.012	0.0658	0.0009	0.3824	410	5	416	9	98.5
RS-14-16_M06c	767	0.0558	0.0008			0.508	0.010	0.0661	0.0008	0.5603	413	5	416	7	99.1
RS-14-16_M07c	771	0.0555	0.0011			0.506	0.012	0.0662	0.0008	0.3859	413	5	416	8	99.4
RS-14-16_M15c	333	0.0561	0.0012			0.511	0.012	0.0663	0.0008	0.2726	414	5	418	8	98.9
RS-14-16_M04c	778	0.0563	0.0010			0.515	0.011	0.0663	0.0008	0.3982	414	5	422	7	98.1
RS-14-16_M11	111	0.0558	0.0010			0.509	0.011	0.0665	0.0008	0.3196	415	5	418	7	99.3
RS-14-16_M16c	361	0.0569	0.0010			0.519	0.011	0.0665	0.0008	0.4282	416	5	424	8	98.1
RS-14-16_M14	340	0.0549	0.0009			0.503	0.011	0.0665	0.0008	0.5440	415	5	413	8	100.5
RS-14-16_M03c	827	0.0560	0.0009			0.514	0.011	0.0666	0.0008	0.5172	416	5	420	7	98.9
RS-14-16_M09c	965	0.0557	0.0011			0.514	0.012	0.0673	0.0008	0.3350	420	5	421	8	99.8

RS-14-16_M10	182	0.0553	0.0010			0.513	0.011	0.0675	0.0008	0.2777	421	5	420	8	100.2
RS-14-16_M12c	181	0.0571	0.0017			0.530	0.016	0.0675	0.0013	0.2515	421	8	431	11	97.7
RS-14-16_M02c	982	0.0554	0.0009			0.516	0.011	0.0678	0.0008	0.4345	423	5	422	7	100.3
RS-14-16_M05c	1321	0.0555	0.0043			0.503	0.037	0.0682	0.0016	0.0263	425	10	405	25	104.7
RS-14-16_M08c	462	0.0552	0.0028			0.514	0.026	0.0682	0.0012	0.0141	425	7	415	18	102.4
Standards															
Run D and C															
Bananeiro 1	3577	0.0587	0.0013	0.02565	0.00057	0.656	0.028	0.0808	0.0038	0.3649	501	11	511	9	97.8
Bananeiro 2	3570	0.0598	0.0015	0.02582	0.00065	0.668	0.036	0.0811	0.0040	0.4049	503	12	517	11	97.1
Itambe 3	3076	0.0576	0.0016	0.02771	0.00083	0.635	0.038	0.0808	0.0040	0.4493	501	12	496	12	101.0
Itambe 4	3059	0.0576	0.0015	0.02659	0.00070	0.631	0.034	0.0804	0.0040	0.3452	498	12	495	10	100.6
Bananeiro 3	3680	0.0583	0.0013	0.02575	0.00060	0.636	0.058	0.0796	0.0072	0.3951	494	43	499	35	98.8
Bananeiro 4	3660	0.0590	0.0014	0.02607	0.00062	0.639	0.058	0.0788	0.0071	0.4079	489	43	501	37	97.5
Itambe 5	3203	0.0589	0.0017	0.02680	0.00084	0.635	0.059	0.0784	0.0071	0.4030	486	43	499	35	97.4
Itambe 6	3064	0.0588	0.0014	0.02821	0.00085	0.639	0.059	0.0787	0.0071	0.4366	488	43	500	36	97.5
KMO 1	4710	0.1124	0.0014	0.10450	0.00300	4.830	0.150	0.3124	0.0144	0.6629	1751	35	1786	13	98.0
KMO 2	2738	0.1120	0.0018	0.10120	0.00340	4.782	0.152	0.3130	0.0144	0.4677	1756	36	1778	13	98.7
KMO 3	4970	0.1118	0.0015	0.10900	0.00300	4.846	0.138	0.3147	0.0148	0.5728	1762	36	1790	12	98.4
KMO 4	2771	0.1129	0.0015	0.10380	0.00370	4.868	0.160	0.3154	0.0150	0.6536	1765	36	1793	14	98.4
KMO 5	2809	0.1132	0.0017	0.10250	0.00340	4.931	0.164	0.3153	0.0150	0.5919	1765	37	1804	14	97.8
KMO 6	4860	0.1122	0.0013	0.10460	0.00330	4.752	0.420	0.3078	0.0280	0.6933	1728	140	1774	74	97.3
KMO 7	2881	0.1127	0.0014	0.10230	0.00330	4.842	0.430	0.3132	0.0280	0.6440	1755	140	1789	75	98.1
KMO 8	4650	0.1126	0.0012	0.10500	0.00320	4.739	0.420	0.3061	0.0280	0.7489	1720	140	1771	74	97.0
KMO 9	2888	0.1132	0.0013	0.10260	0.00320	4.887	0.440	0.3127	0.0280	0.6818	1752	140	1797	75	97.4
KMO 10	2858	0.1138	0.0014	0.10200	0.00330	4.973	0.440	0.3173	0.0290	0.6558	1775	140	1812	76	97.9
Trebil 1	5080	0.0518	0.0016	0.01368	0.00024	0.307	0.009	0.0435	0.0010	0.1776	274	6	270	7	101.4
Trebil 2	5220	0.0517	0.0014	0.01363	0.00024	0.306	0.009	0.0434	0.0010	0.1343	274	6	270	7	101.3
Trebil 3	5060	0.0516	0.0015	0.01335	0.00023	0.308	0.009	0.0436	0.0011	0.2900	275	7	272	7	101.3
Trebil 4	5180	0.0519	0.0017	0.01355	0.00026	0.306	0.009	0.0425	0.0010	0.2018	268	6	270	7	99.3
Trebil 5	4870	0.0516	0.0017	0.01332	0.00026	0.305	0.010	0.0427	0.0010	0.2874	269	6	271	8	99.3
Trebil 6	5070	0.0518	0.0014	0.01352	0.00024	0.308	0.008	0.0434	0.0010	0.1966	274	6	272	6	100.7
Trebil 7	5050	0.0517	0.0014	0.01355	0.00025	0.307	0.009	0.0430	0.0010	0.2772	271	6	271	7	100.2
Trebil 8	5170	0.0514	0.0015	0.01343	0.00024	0.305	0.009	0.0420	0.0010	0.2421	265	6	269	7	98.4
Trebil 9	4970	0.0516	0.0013	0.01343	0.00023	0.308	0.008	0.0433	0.0010	0.3973	273	6	272	7	100.2
Trebil 10	5160	0.0514	0.0015	0.01360	0.00027	0.306	0.010	0.0426	0.0010	0.3723	269	6	270	8	99.6
Trebil 11	4950	0.0517	0.0015	0.01349	0.00024	0.307	0.009	0.0436	0.0010	0.2473	275	6	271	7	101.4
Trebil 12	5100	0.0518	0.0015	0.01334	0.00023	0.307	0.009	0.0436	0.0010	0.1799	275	7	271	7	101.6
Trebil 13	5080	0.0518	0.0015	0.01342	0.00024	0.307	0.009	0.0432	0.0010	0.2702	272	6	271	7	100.7
Trebil 14	4980	0.0517	0.0014	0.01368	0.00024	0.306	0.008	0.0431	0.0010	0.2645	272	6	270	7	100.7
Trebil 15	5030	0.0515	0.0018	0.01346	0.00027	0.308	0.011	0.0434	0.0010	0.3266	274	6	272	9	100.8
Trebil 16	5220	0.0519	0.0015	0.01349	0.00024	0.308	0.009	0.0431	0.0010	0.2486	272	6	272	7	100.2
Trebil 17	5140	0.0518	0.0014	0.01364	0.00024	0.306	0.009	0.0428	0.0010	0.2594	270	6	270	7	100.1
Trebil 18	5180	0.0519	0.0013	0.01347	0.00023	0.307	0.028	0.0431	0.0039	0.4918	272	24	271	22	100.3
Trebil 19	5070	0.0516	0.0013	0.01359	0.00024	0.303	0.028	0.0427	0.0039	0.3248	270	24	268	22	100.7
Trebil 20	4990	0.0517	0.0014	0.01348	0.00026	0.304	0.028	0.0426	0.0039	0.3903	269	24	268	22	100.2
Trebil 21	4940	0.0517	0.0014	0.01343	0.00023	0.300	0.028	0.0423	0.0038	0.3011	267	24	266	22	100.3
Trebil 22	5140	0.0516	0.0015	0.01346	0.00021	0.301	0.028	0.0426	0.0039	0.2753	269	24	266	22	101.0
Trebil 23	5090	0.0517	0.0015	0.01359	0.00023	0.297	0.027	0.0418	0.0038	0.2353	264	23	264	22	100.0
Trebil 24	5100	0.0518	0.0013	0.01353	0.00022	0.337	0.031	0.0473	0.0043	0.4092	298	26	294	24	101.3
Trebil 25	5090	0.0516	0.0014	0.01351	0.00025	0.304	0.028	0.0423	0.0038	0.3639	267	24	268	22	99.5
Trebil 26	5100	0.0517	0.0014	0.01346	0.00021	0.341	0.032	0.0482	0.0044	0.4536	303	27	297	24	102.0
Trebil 27	5070	0.0513	0.0013	0.01344	0.00025	0.300	0.028	0.0424	0.0038	0.3589	267	24	265	22	100.8
Trebil 28	5050	0.0518	0.0015	0.01375	0.00024	0.308	0.029	0.0432	0.0039	0.3412	273	24	271	22	100.4
Trebil 29	5020	0.0518	0.0014	0.01338	0.00025	0.309	0.029	0.0432	0.0039	0.3581	273	24	272	22	100.3
Trebil 30	4990	0.0521	0.0014	0.01342	0.00022	0.309	0.028	0.0431	0.0039	0.3606	272	24	273	22	99.7
Trebil 31	5220	0.0517	0.0013	0.01345	0.00021	0.302	0.028	0.0426	0.0039	0.3930	269	24	268	21	100.4
Trebil 32	5040	0.0517	0.0015	0.01339	0.00021	0.302	0.028	0.0424	0.0039	0.4074	268	24	267	22	100.3
Trebil 33	5020	0.0515	0.0013	0.01357	0.00025	0.304	0.028	0.0430	0.0039	0.3070	271	24	269	22	100.8
Trebil 34	5120	0.0517	0.0013	0.01370	0.00027	0.304	0.028	0.0427	0.0039	0.3747	269	24	269	22	100.1
Run B															
Bananeiro 1	3761	0.0587	0.0010			0.651	0.014	0.0808	0.0009	0.3797	501	5	508	8	98.5
Bananeiro 2	3722	0.0603	0.0010			0.677	0.014	0.0817	0.0010	0.4021	506	6	524	9	96.4
Bananeiro 3	3791	0.0589	0.0010			0.657	0.014	0.0806	0.0009	0.4299	500	6	512	9	97.6
Itambe 1	3107	0.0573	0.0012			0.637	0.015	0.0810	0.0011	0.3055	502	6	501	9	100.2
Itambe 2	3054	0.0580	0.0011			0.640	0.015	0.0807	0.0010	0.3710	500	6	501	9	99.9
Itambe 3	2981	0.0578	0.0010			0.640	0.013	0.0804	0.0010	0.3502	499	6	501	8	99.5
KMO 1	2807	0.1127	0.0014			5.069	0.091	0.3263	0.0040	0.6791	1819	19	1829	15	99.5
KMO 2	3082	0.1210	0.0020			5.000	0.150	0.2985	0.0059	0.8771	1681	29	1808	26	92.4
KMO 3	2895	0.1118	0.0014			4.852	0.085	0.3152	0.0034	0.6219	1767	17	1792	15	98.6
KMO 4	2792	0.1124	0.0014			4.909	0.084	0.3180	0.0035	0.6343	1779	17	1804	15	98.6
KMO 5	2885	0.1115	0.0014			4.855	0.085	0.3162	0.0033	0.5606	1771	16	1793	15	98.8
KMO 6	2952	0.1120	0.0013			4.934	0.087	0.3195	0.0036	0.7018	1786	17	1806	15	98.9
Trebil 1	5008	0.0515	0.0009			0.307	0.007	0.0434	0.0005	0.3285	274	3	272	5	100.7
Trebil 2	5057	0.0515	0.0009			0.308	0.007	0.0433	0.0005	0.4369	273	3	272	5	100.3
Trebil 3	5129	0.0518	0.0010			0.309	0.007	0.0432	0.0006	0.4133	272	3	273	6	99.9
Trebil 4	5124	0.0519	0.0011			0.307	0.008	0.0428	0.0005	0.3314	270	3	271	6	99.7

Trebil 5	5143	0.0526	0.0010	0.311	0.007	0.0431	0.0005	0.3553	272	3	275	6	98.9
Trebil 6	4986	0.0511	0.0010	0.302	0.007	0.0430	0.0005	0.3533	271	3	268	5	101.4
Trebil 7	5051	0.0517	0.0011	0.305	0.007	0.0430	0.0005	0.2457	271	3	270	6	100.5
Trebil 8	5040	0.0524	0.0010	0.309	0.007	0.0431	0.0005	0.4162	272	3	274	5	99.4
Trebil 9	5108	0.0519	0.0010	0.307	0.007	0.0430	0.0005	0.3295	272	3	271	5	100.1
Trebil 10	5186	0.0514	0.0010	0.303	0.007	0.0427	0.0005	0.2736	270	3	268	5	100.6
Trebil 11	5063	0.0516	0.0010	0.307	0.007	0.0435	0.0005	0.2110	274	3	272	5	100.9
Trebil 12	5045	0.0510	0.0010	0.300	0.007	0.0428	0.0005	0.3496	270	3	266	5	101.5
Trebil 13	5048	0.0519	0.0010	0.310	0.007	0.0434	0.0005	0.3557	274	3	274	6	100.0
Trebil 14	5063	0.0521	0.0010	0.310	0.007	0.0431	0.0005	0.3848	272	3	273	6	99.5
Trebil 15	5148	0.0515	0.0010	0.306	0.007	0.0432	0.0006	0.4290	273	3	271	5	100.6
Trebil 16	4975	0.0519	0.0010	0.307	0.007	0.0428	0.0005	0.2913	270	3	271	6	99.5
Trebil 17	5181	0.0522	0.0011	0.310	0.007	0.0432	0.0005	0.3129	273	3	274	6	99.5
Trebil 18	4988	0.0513	0.0010	0.307	0.007	0.0434	0.0005	0.3302	274	3	271	5	100.9

acorrected for background, instrumental drift and mass bias fractionation based on primary stantard.

c rho is the 207Pb/235U/206Pb/238U error correlation coefficient.

d degree of concordance: 100-((1+((206Pb/238U - 207Pb/235U)/206Pb/238U)) x 100)

Table DR5

Sample	$^{173}Yb/^{171}Yb$	±	$^{176}Hf/^{177}Hf$	±	$^{178}Hf/^{177}Hf$	±	$^{179}Hf/^{177}Hf$	±	$^{176}Hf/^{177}Hf$	±	$^{178}Hf/^{177}Hf$	±	$^{176}Lu/^{177}Hf$	±	$^{176}Yb/^{177}Hf$	±	f ^{176}Yb	Yb/Hf	total Hf (v)	**Age (Ma) [a]**	**$^{176}Hf/^{177}Hf_{(t)}$**	**$\varepsilon Hf_{(t)}$ [b]**	**±2s**	**T_{DM} [c] (Ga)**
1	1.147219	0.000034	0.494753	0.002564	1.477620	0.000018	0.742847	0.000010	0.282730	0.000014	1.467273	0.000016	0.006020	0.000061	0.209964	0.002531	0.4170	0.295600	17	502.7	0.282673	7.25	1.00	1.05
2	1.149428	0.000041	0.444767	0.000943	1.479240	0.000020	0.744385	0.000010	0.282795	0.000014	1.467360	0.000018	0.004483	0.000022	0.161496	0.000929	0.3587	0.226438	15	502.7	0.282752	10.06	0.98	0.88
3	1.149734	0.000056	0.419552	0.001942	1.479336	0.000023	0.744516	0.000013	0.282768	0.000016	1.467325	0.000021	0.003811	0.000047	0.136904	0.001913	0.3193	0.191662	10	502.7	0.282732	9.34	1.11	0.92
4	1.149518	0.000066	0.426506	0.001087	1.479175	0.000035	0.744447	0.000013	0.282774	0.000015	1.467235	0.000033	0.003974	0.000027	0.143764	0.001068	0.3322	0.201308	10	502.7	0.282736	9.50	1.08	0.91
5	1.149804	0.000066	0.472800	0.005560	1.479215	0.000028	0.744430	0.000015	0.282815	0.000018	1.467291	0.000026	0.005209	0.000126	0.189172	0.005503	0.3869	0.264989	13	502.7	0.282766	10.54	1.24	0.85
6	1.149565	0.000066	0.453926	0.001167	1.479191	0.000036	0.744402	0.000019	0.282777	0.000022	1.467295	0.000032	0.004697	0.000022	0.170614	0.001160	0.3715	0.239086	13	502.7	0.282732	9.35	1.54	0.92
7	1.148999	0.000040	0.548196	0.001977	1.478885	0.000021	0.744144	0.000012	0.282786	0.000020	1.467246	0.000020	0.007389	0.000052	0.263260	0.001942	0.4733	0.369054	11	502.7	0.282716	8.78	1.41	0.96
8	1.148986	0.000033	0.636235	0.002264	1.478859	0.000023	0.744091	0.000013	0.282740	0.000020	1.467273	0.000019	0.009608	0.000052	0.350146	0.002232	0.5428	0.490807	10	502.7	0.282650	6.43	1.40	1.10
9	1.148894	0.000043	0.541450	0.003300	1.478767	0.000023	0.743976	0.000013	0.282707	0.000019	1.467295	0.000019	0.007392	0.000072	0.256440	0.003263	0.4642	0.359602	11	502.7	0.282638	6.00	1.33	1.13
10	1.148338	0.000055	0.539267	0.002125	1.478514	0.000031	0.743756	0.000018	0.282808	0.000020	1.467261	0.000026	0.007053	0.000047	0.254329	0.002100	0.4649	0.357012	12	502.7	0.282741	9.67	1.44	0.90
11	1.148485	0.000066	0.444908	0.004467	1.478539	0.000031	0.743779	0.000013	0.282774	0.000015	1.467264	0.000030	0.004731	0.000118	0.161346	0.004397	0.3430	0.226403	11	502.7	0.282729	9.23	1.07	0.93

(a) Concordia age

(b) Initial $^{176}Hf/^{177}Hf$ and eHf calculated using the estimated Pb-Pb ages of respective zircon domains, and the CHUR parameters:
$^{176}Lu/^{177}Hf$ = 0.0336, and $^{176}Hf/^{177}Hf$ = 0.282785 (Bouvier et al., 2008).;

(c) two stage model age in billion years using the measured $^{176}Lu/^{177}Lu$ and the estimated Pb/Pb age (first stage), a value of 0.015 for the average continental crust (second stage), and a depleted mantle $^{176}Lu/^{177}Hf$ and $^{176}Hf/^{177}Hf$ of 0.03933 and 0.283294 (Blichert-Toft & Puchtel, 2010).

Standards	$^{173}Yb/^{171}Yb$	±	$^{176}Hf/^{177}Hf$	±	$^{178}Hf/^{177}Hf$	±	$^{179}Hf/^{177}Hf$	±	$^{176}Hf/^{177}Hf$	±	$^{178}Hf/^{177}Hf$	±	$^{176}Lu/^{177}Hf$	±	$^{176}Yb/^{177}Hf$	±	f ^{176}Yb	Yb/Hf	total Hf (v)	**Average $^{176}Hf/^{177}Hf$**	**±1s**	**±2s**	**Published values $^{176}Hf/^{177}Hf$**	**±2s**
Mudtank	1.141941	0.005983	0.281259	0.000008	1.477593	0.000032	0.742811	0.000013	0.282533	0.000012	1.467281	0.000030	0.000019	0.0000001	0.000706	0.000007	0.0025	0.000993	11	0.282517	10	69	0.282504	44
	1.139893	0.003757	0.281561	0.000007	1.476064	0.000023	0.741639	0.000014	0.282537	0.000009	1.466923	0.000020	0.000019	0.0000001	0.000774	0.000005	0.0027	0.001097	15					
	1.142130	0.004784	0.281007	0.000007	1.479365	0.000021	0.744569	0.000012	0.282507	0.000010	1.467302	0.000019	0.000019	0.0000001	0.000812	0.000007	0.0029	0.001142	11					
	1.149749	0.003212	0.281086	0.000006	1.479085	0.000019	0.744272	0.000010	0.282499	0.000008	1.467318	0.000017	0.000019	0.0000001	0.000839	0.000005	0.0030	0.001175	16					
	1.141415	0.005146	0.281387	0.000009	1.476964	0.000041	0.742308	0.000011	0.282510	0.000010	1.467155	0.000043	0.000019	0.0000001	0.000768	0.000007	0.0027	0.001085	14					
Plesovice	1.149829	0.000483	0.289152	0.000015	1.479028	0.000024	0.744197	0.000013	0.282454	0.000012	1.467335	0.000020	0.000171	0.0000002	0.008877	0.000014	0.0304	0.012430	11	0.282481	10	68	0.282482	13
	1.146602	0.000878	0.284963	0.000035	1.477856	0.000025	0.743046	0.000012	0.282492	0.000011	1.467310	0.000023	0.000092	0.0000006	0.004453	0.000034	0.0155	0.006266	11					
	1.148643	0.000569	0.284715	0.000016	1.479495	0.000020	0.744665	0.000010	0.282479	0.000008	1.467336	0.000019	0.000084	0.0000003	0.004538	0.000015	0.0158	0.006370	18					
	1.147783	0.000272	0.288397	0.000007	1.478002	0.000019	0.743200	0.000010	0.282469	0.000007	1.467302	0.000018	0.000152	0.0000001	0.007907	0.000006	0.0272	0.011125	20					
	1.148155	0.001328	0.285167	0.000019	1.479149	0.000116	0.744039	0.000019	0.282500	0.000012	1.467612	0.000126	0.000098	0.0000004	0.004804	0.000015	0.0167	0.006736	10					
	1.147497	0.000464	0.286124	0.000011	1.478767	0.000021	0.743931	0.000010	0.282489	0.000009	1.467339	0.000019	0.000112	0.0000003	0.005779	0.000010	0.0200	0.008129	18					
	1.149098	0.000372	0.287573	0.000007	1.479008	0.000018	0.744203	0.000011	0.282487	0.000009	1.467310	0.000016	0.000138	0.0000002	0.007271	0.000005	0.0250	0.010204	18					
	1.146854	0.000553	0.287754	0.000009	1.478396	0.000020	0.743574	0.000012	0.282480	0.000011	1.467324	0.000018	0.000143	0.0000002	0.007340	0.000008	0.0252	0.010324	12					
Temora	1.148982	0.000204	0.300328	0.000327	1.478861	0.000022	0.744013	0.000013	0.282667	0.000010	1.467351	0.000018	0.000543	0.0000080	0.019538	0.000322	0.0641	0.027412	13	0.282649	20	139	0.28268	31
	1.146803	0.000148	0.340386	0.000242	1.477710	0.000043	0.742858	0.000020	0.282680	0.000020	1.467351	0.000035	0.001677	0.0000043	0.058701	0.000240	0.1705	0.082513	8					
	1.147523	0.000125	0.319794	0.000126	1.477376	0.000025	0.742809	0.000015	0.282659	0.000014	1.467068	0.000021	0.001164	0.0000017	0.038376	0.000125	0.1187	0.053926	9					
	1.146257	0.000425	0.312260	0.000228	1.476786	0.000140	0.742602	0.000030	0.282589	0.000034	1.466687	0.000135	0.000864	0.0000044	0.031119	0.000218	0.0985	0.043762	8					